Siemens PTI Report Number: R116-14

Subsynchronous Resonance Screening Study for the PJM Regional Transmission Expansion Plan

Prepared for

PJM Interconnection, LLC

Submitted by:
James W. Feltes Senior Manager, Consulting
Ram Nath, Principal Consultant
Rajat Majumder, Senior Staff Consultant

Rev. [1]
January 16, 2015

Siemens PTI Project Number P/23-115248

Siemens Industry, Inc.
Siemens Power Technologies International
400 State Street • P.O. Box 1058
Schenectady, New York 12301-1058 USA
Tel: +1 (518) 395-5000 • Fax: +1 (518) 346-2777
www.siemens.com/power-technologies

Revision History

Date	Rev.	Description
January 6, 2015	0	Draft Report
January 16, 2015	0	Final Report
January 16, 2015	1	Final Report incorporating PJM’s comments on Rev 0.

Contents

Legal Notice

This page intentionally left blank.

Executive Summary

In response to a request by PJM for potential projects to mitigate the Artificial Island (AI) system performance issues, Dominion Virginia Power has proposed to install two Thyristor Controlled Series Compensators (TCSCs) as well as a Static Var Compensator (SVC). Series compensation in the vicinity of large power plants raises concerns about the potential for subsynchronous resonance (SSR) interaction. Thus PJM is interested in determining the SSR vulnerability of the Salem Unit 1, Salem Unit 2, and Hope Creek turbo-generating units in the AI due to the proposed installation of TCSCs on the Salem - New Freedom 500 kV and Hope Creek - New Freedom 500 kV lines.

Series capacitors provide many benefits to improve the transmission capability of long transmission lines as well as to enhance generator transient stability. However, the presence of series capacitors in a power system may also cause an adverse interaction between the torsional vibrations of the nearby turbo-generating units and the current oscillations in the connected network. This phenomenon is referred to as subsynchronous resonance (SSR). The dangerous impact of this phenomenon was first noticed in the destruction of the generator shafts at the Mohave Power Station (California, USA) on December 9, 1970, and again on October 26, 1971. Since then, considerable effort has been made to analyze the phenomenon and seek ways to prevent future damages.

The main objective of this study was to determine whether the proposed TCSC installation has the potential to create a SSR condition with the AI generating units.

Siemens PTI developed a detailed model of the PJM network around the AI generating units in the PSCAD simulation program. The model was validated by comparing the steady state power flow, short circuit levels and transient stability results to those of the full PJM load flow and stability models. The network model included the two TCSCs with their firing logic on the Hope Creek - New Freedom and the Salem – New Freedom lines. The PSCAD network model was enhanced to incorporate a rotor shaft representation of the AI turbo-generating units to enable the investigation of the potential for SSR related to the addition of the two TCSCs.

Several contingency scenarios were created that result in a radial connection of the AI generating units to the TCSC lines. Such radial connections are the operating conditions that are most likely to exhibit SSR.

Detailed simulation studies were performed for the proposed project to calculate the damping of torsional oscillations that could be experienced by the AI units. The damping was evaluated for each of the rotor natural frequencies of the Salem Unit 1 and Salem Unit 2, and for a range of frequencies for the Hope Creek unit (its rotor natural frequencies were not supplied).

It has been found that with a set of TCSC parameters developed by Siemens PTI, the system with the TCSCs does not provide positive damping for all subsynchronous frequencies and hence shows the potential for SSR.

The study results for the Salem Unit 1 show that the electrical damping is positive for the rotor natural frequencies below [redacted] However, the Salem Unit 1 experiences negative damping characteristics for rotor frequencies of [redacted] These observations are made for both operating scenarios evaluated, i.e., Salem Unit 1 radial with 5023 and 5024, and Salem Unit 1 radial with 5024. It should be further noted that when Salem Unit 1 was radial with two compensated lines, the peak amplitude of the torque is as high as 5 pu as compared to 1.5 pu in the scenario with only one compensated line.

The study results for the Salem Unit 2 show a positive damping for rotor natural frequencies of [redacted] The damping for the rotor frequencies of [redacted] is a very small positive damping. The coupling torque between the turbine and the rotor masses for the rotor frequencies of [redacted] exhibits sustained oscillations with practically no damping. While the study scenario of Salem Unit 2 radial with 2 TCSC lines show a very small positive damping for a rotor resonance frequency of [redacted] the study scenario of Salem Unit 2 radial with 5024 shows a negative damping for the same rotor resonance frequency.

As noted above, the rotor natural frequencies for the Hope Creek unit were not supplied so a range of frequencies was analyzed. The study results for the Hope Creek unit show positive damping for rotor frequencies below [redacted] The electrical damping observed is very small for frequencies between [redacted] The Hope Creek unit experiences negative damping for rotor frequencies higher than [redacted]. The negative damping is significantly higher for a rotor frequency of [redacted] for the scenario of Hope Creek unit radial with 5023 and 5024 and for the rotor frequency of [redacted] for the scenario of Hope Creek unit radial with 5023 only.

The study results have shown that the generating units at the Artificial Islands can be subjected to SSR phenomenon when a TCSC is employed as presently proposed by Dominion. Since detailed design parameters were not supplied by Dominion, it was necessary to develop TCSC parameters and firing angle logic to meet the fundamental frequency specifications. Those parameters satisfy the design criteria available in the technical literature. More detailed design analysis by a manufacturer may be able to develop parameters and controls that are less susceptible to SSR, but the initial investigations performed in this analysis could not determine parameters and controls that would result in adequate damping over the entire frequency range of concern and for all potential operating conditions.

Note that the study did not consider a subsynchronous damping controller (SSDC). An SSDC could have a significant impact on the damping of SSR oscillations and could potentially remedy the concerns seen in the simulations performed. The impact of an SSDC should be evaluated if such a controller can be implemented as part of the proposed TCSCs.

Therefore if this project is to proceed, Siemens PTI recommends that PJM have a discussion with Dominion Virginia Power and further engage the prospective manufacturers to develop TCSC designs, possibly with an SSDC, that will mitigate SSR and provide adequate damping over the entire frequency range of concern and for all potential operating conditions.

Analysis such as the one performed in this study would be required to investigate the effectiveness of any revised proposal.

Section

1

Introduction

In response to a request by PJM for potential projects to mitigate the Artificial Island (AI) system performance issues, Dominion Virginia Power has proposed to install two Thyristor Controlled Series Compensators (TCSCs) as well as a Static Var Compensator (SVC). Series compensation in the vicinity of large power plants raises concerns about the potential for subsynchronous resonance (SSR) interaction. Thus PJM is interested in determining the SSR vulnerability of the Salem Unit 1, Salem Unit 2, and Hope Creek turbo-generating units in the AI due to the proposed installation of TCSCs on the Salem - New Freedom 500 kV and Hope Creek - New Freedom 500 kV lines.

Series capacitors provide many benefits to improve the transmission capability of long transmission lines as well as to enhance generator transient stability. However, the presence of series capacitors in a power system may also cause an adverse interaction between subsynchronous oscillatory modes within different sections of the shafts of nearby turbo-generating units and the connected network's resonant frequencies. This phenomenon is referred to as subsynchronous resonance (SSR). The dangerous impact of this phenomenon was first noticed in the destruction of the generator shafts at the Mohave Power Station (California, USA) on December 9, 1970, and again on October 26, 1971. Since then, considerable effort has been made to analyze the phenomenon and seek ways to prevent future damages.

The main objective of this study is to determine whether the proposed TCSC solution has the potential to create a SSR condition with the AI generating units.

This page intentionally left blank.

Section
2

System Data and Assumptions

The following data and related information was provided to Siemens PTI for this project:

Modeling Data

The following data was provided:

1. **Base Power Flow Case**: This case has all lines in service with the AI units at maximum real power output. This case has been developed based on the NERC MMWG 2011 Series 2017 Summer Light Load case in PSS®E version 32

2. **Dynamic Case**: This case has been developed based on the NERC SSDWG 2011 Series 2017 Summer Light Load case in PSS®E version 32

3. **Short Circuit Case**: This case has a 2017 short circuit model in PSS®E version 32 and ASPEN *.olr format. (separate file)

4. **Contingency List**

5. **Fault Clearing Times**

6. **One-Line Diagram of the Artificial Island Area**

7. **Torsional Data of the AI generating Units**: The mass moment of inertia of the individual rotor masses were provided for the Salem Unit 1 and Salem Unit 2 as given in Table 2-1 and Table 2-2 respectively. The mass moment of inertias for the Hope Creek generating unit were available for the turbine and the generating unit as two masses. These values are tabulated in Table 2-3. The torsional modes for the Salem Unit 1 and Salem Unit 2 were also made available. These modes are shown in Table 2-4 and Table 2-5 respectively. The torsional modes of the Hope Creek generating unit were not available.

Table 2-1. Mass Moment of Inertia of Salem Unit 1 Rotor Masses

Rotor Mass	Mass Moment of Inertia kg*m^2
HP Turbine	[redacted]
LP1 Turbine	
Jackshaft 1	
LP2 Turbine	
Jackshaft 2	
LP3 Turbine	
Generator	
Exciter	
Total	

Table 2-2. Mass Moment of Inertia of Salem Unit 2 Rotor Masses

Rotor Mass	Mass Moment of Inertia kg*m^2
HP Turbine	[redacted]
LP1 Turbine	
Jackshaft 1	
LP2 Turbine	
Jackshaft 2	
LP3 Turbine	
Generator	
Exciter	
Total	

Table 2-3. Mass Moment of Inertia of Hope Creek unit Rotor Masses

Rotor Mass	Mass Moment of Inertia lb*ft^2
Turbine	[redacted]
Generator and Exciter	

Table 2-4. Torsional Modes of Salem Unit 1

Mode	Rotor Frequency Hz
1	[redacted]
2	
3	
4	
5	
6	
7	

Table 2-5. Torsional Modes of Salem Unit 2

Mode	Rotor Frequency Hz
1	[redacted]
2	
3	
4	
5	

This page intentionally left blank.

Section

3

Subsynchronous Resonance Phenomena and Modeling Approach

3.1 Fundamentals of Subsynchronous Resonance

The rotor of a turbo generator is a complex mechanical system. The rotor contains various turbine shaft sections such as high pressure, intermediate pressure and low pressure turbine sections. Other sections include the generator rotor windings and the rotor of the brushless excitation system. Such a rotor system typically has a large number of torsional vibration modes both above and below the synchronous frequency. However the main issue arises primarily in the subsynchronous frequency range where these torsional modes can interact with the electrical system. This phenomenon is known as Subsynchronous Resonance (SSR). For evaluating such phenomenon the rotor is typically represented by a number of lumped mass sections connected through various coupling constants as shown in Figure 3-1.

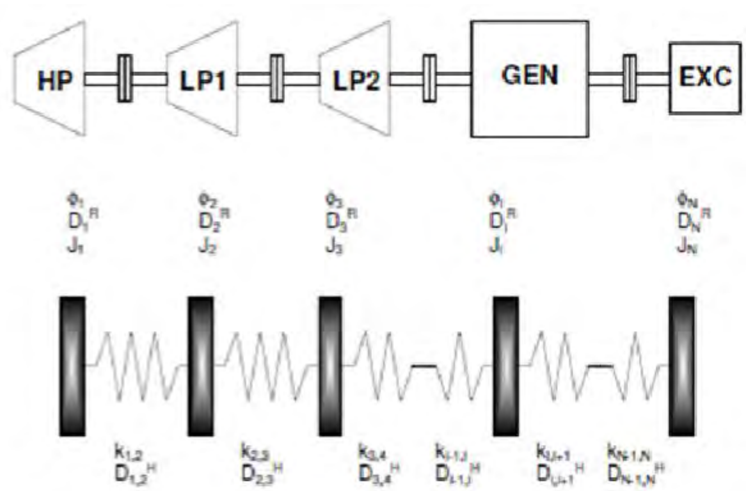

Figure 3-1. Multi-Mass Rotor Model

The currents in the generator three-phase stator windings are normally sinusoidal with 120° phase displacement – in time and space with respect to each pole pair. During the presence of electrical resonant voltages however, they form a component at system frequency and one below system frequency. Similarly, the rotating field B_{stator} generated by these currents also has two components: the steady-state main flux component with the amplitude B_{main} and the resonant component with the amplitude $B_{resonance}$:

$$B_{stator} = B_{main} \sin(2\pi f_0 t - \alpha_0) + B_{resonance} \sin(2\pi f_{resonance} t - \beta_0)$$

The second term rotates in the air gap of the machine at the angular frequency $2\pi_{fresonance}$ which is lower than the mechanical speed of the shaft $2\pi f0$ (for a 2-pole synchronous machine). The subsynchronous magneto-motive force (MMF) induced in the stator windings causes a corresponding rotor MMF which, according to Lenz's Law, opposes the stator field. It therefore has the same subsynchronous frequency $f_{resonance}$. However, relative to the rotor speed, it rotates with the frequency $f_{torque} = | f_{resonance} - f0 | = | f0 - f_{resonance} |$. The rotor MMF interacts with the resonant stator MMF and produces an asynchronous torque component at frequency ftorque, a phenomenon known as the induction generator effect. The generator response to this additional flux component is comparable to that of an induction machine operating in the generation region with negative slip
$s = (f_{resonance} - f0) / f_{resonance}$.

The asynchronous torque component acts on the shaft system of the turbine-generator and excites subsynchronous torsional oscillations. The shaft system of a turbine-generator unit can be represented as a multi-mass-spring oscillating system. In Table 3-1 the individual masses represent the sections of the turbine, the generator and the exciter.

J	inertia constant
k	torsional stiffness constant
D^R	speed-proportional frictional damping
D^H	hysteresis damping, proportional to the turning speed differential
φ	torque angle

[redacted]

Figure 3-2. Mode Shapes

The overall rotor structure has a number of oscillatory modes, that is, natural frequencies of oscillation. As shown in Figure 3-2, one can see a number subsynchronous and supersynchronous modes and their shapes. The mode shapes (right eigenvectors) show the relative contribution of various states (angular displacement of various sections) within the different oscillatory modes. In the example provided here, the shaft system has a natural frequency at [redacted], at which the low pressure section LP2 is in complete phase opposition to the other sections. Once excited with this frequency it would swing against the rest of the shaft sections and therefore cause stresses mostly on the couplings to the left and right of this section. This example demonstrates that if the frequency f_{torque} of the subsynchronous electrical torque is near one of the natural shaft frequencies f_{mj}, and if its component in phase with the rotor speed deviation exceeds the inherent damping torque of the rotating system, subsynchronous resonance occurs. The torque oscillations can then rapidly increase and may cause severe damage to the shaft (e.g., Figure 3-3 and Figure 3-4).

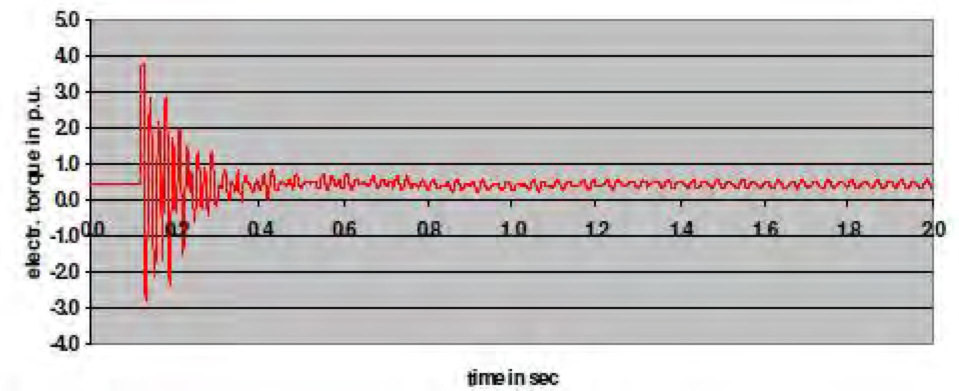

Figure 3-3. Generator Air Gap Torque following a 3 Phase Fault

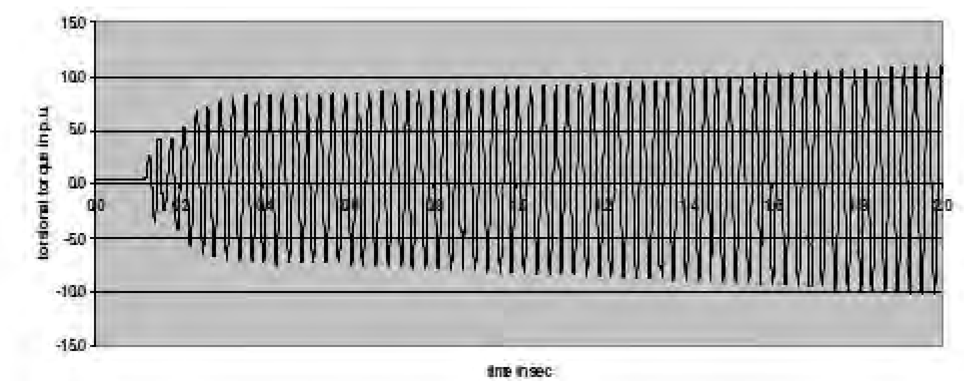

Figure 3-4. Torque between Shaft Sections following a 3 Phase Fault

A simulation platform suitable for computing electromagnetic transients (such as PSCAD) may be used to simulate the transient time response. Such a time-domain simulation uses a full three phase electrical representation of the network and generators, and permits detailed modeling of the multi-mass shaft systems. A detailed representation of nonlinear effects is also possible. SSR can be identified by observing the time response of the torques of a particular shaft system. If the torque oscillations persist or grow in time, then the system almost surely has an SSR problem.

3.2 Two-Mass Modeling Approach

As stated in the Introduction, the complete data sets for the AI unit's turbine-generator shafts including inertia constants and coupling constants were not available for all three generating units (Salem Unit 1 and Salem Unit 2 and Hope Creek unit). However, the shaft torsional frequencies were available. Therefore an approximate two-mass modeling approach was adopted. Rather than modeling the entire shaft and all of its modes, in the two-mass modeling approach the inertia constants and coupling constant are computed to represent one of the shaft natural frequencies. Figure 3-5 shows a two mass shaft system. One mass represents the generator, the other mass the turbine. For Salem Unit 1 and Salem Unit 2, the rotational inertias for various sections were available. The inertias of all the turbine sections were added and represented by the turbine mass and the inertias of the generator and exciter were added and represented by the generator mass. For the Hope Creek unit only the lumped rotational inertias were available and used in a similar manner. The shaft coupling constant was then calculated to get the desired shaft frequency as described below.

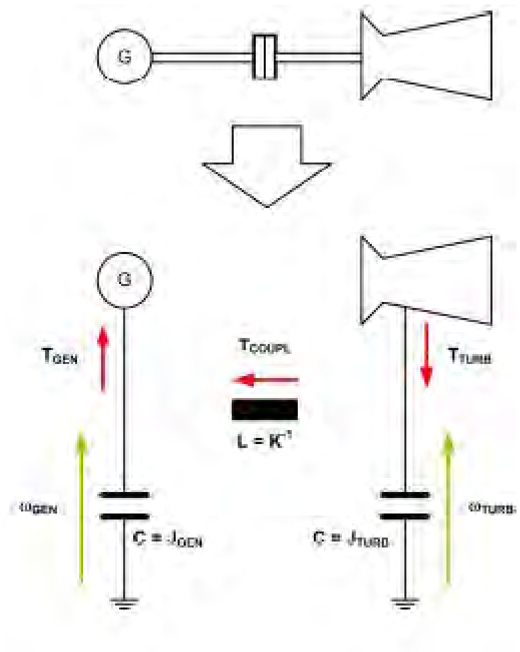

Figure 3-5. Two Mass Model

In Figure 3-5 an equivalent electrical network is shown to represent this two mass mechanical model. The masses are represented by capacitors and torsional stiffness or coupling as a reactor. The two-mass model corresponds to an ordinary differential equation of second order:

$$T = [J]\ddot{\phi} + [K]\phi$$

Here, the J and K are two-by-two matrices of the inertias and stiffness, respectively; φ is the rotor angle of each rotor mass with respect to a reference angle, and T is the torque vector, consisting of the generator air-gap torque and of the turbine torque, i.e. the torques into and out of the shaft system. These two matrices are given by:

$$J = \begin{pmatrix} Jgen & 0 \\ 0 & Jtur \end{pmatrix} \text{ in Kg-m2}$$

and

$$K = \begin{pmatrix} Kcouple & -Kcouple \\ -Kcouple & Kcouple \end{pmatrix} \text{ in Nm/rad}$$

After some algebraic manipulations, the frequency of oscillation is obtained as:

$$Fm = \frac{1}{2\pi}\sqrt{Kcouple\frac{Jgen + Jtur}{Jgen * Jtur}}$$

By choosing the right coupling constant K_{couple}, it is possible to create shaft models representing the entire subsynchronous range of frequencies. The parameters of the two mass models of the AI generating units for the natural modes of oscillations of Salem Unit 1 and Salem Unit 2 are shown in Table A-1 and Table A-2 respectively in Appendix A. The natural modes of oscillations for the Hope Creek generating unit were not supplied. Thus, eleven two mass models were created for subsynchronous frequencies between 5 Hz and 55 Hz at an interval of 5 Hz to cover the range of potential subsynchronous shaft frequencies.

Table 3-1. Two Mass Moment of Inertia of Salem Unit 1

Rotor Mass	Mass Moment of Inertia kg*m^2
Turbine	[redacted]
Generator	

Table 3-2. Two Mass Moment of Inertia of Salem Unit 2

Rotor Mass	Mass Moment of Inertia kg*m^2
Turbine	[redacted]
Generator	

Table 3-3. Two Mass Moment of Inertia of Hope Creek Unit

Rotor Mass	Mass Moment of Inertia kg*m^2
Turbine	[redacted]
Generator	

This page intentionally left blank.

Section

4

Thyristor Controlled Series Capacitor (TCSC) & SSR

4.1 Basic Operations

A thyristor controlled series capacitor is a combination of a conventional series capacitor with a parallel branch consisting of an inductor in series with an anti-parallel thyristors as shown in Figure 4-1. Current commercially operating project examples are the Kayenta TCSC [13] and Slatt TCSC [14] in the US. There are many under commercial operation all around the world. The primary technical benefits derived from such a project are:

- Improved power transfer capacity (increased transient stability margin)
- Damping of power oscillations
- Subsynchronous oscillation mitigation

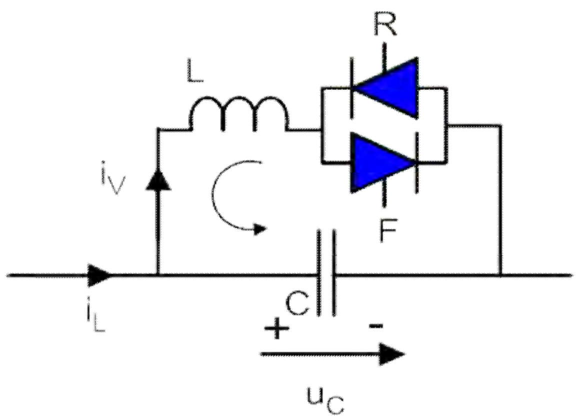

Figure 4-1. TCSC

As seen in Figure 4-1 one component of the TCSC is a thyristor controlled reactor (TCR). There could be three possible modes of operation of such a device.

4.1.1 Thyristor Blocked Mode

In blocked mode, the thyristors are blocked. No firing pulses are provided to the thyristors and as a result the inductor branch acts as an open circuit. In this mode, from the system point of view, the TCSC would appear like a fixed series capacitor. A schematic to demonstrate this mode of operation is shown in Figure 4-2. This is not a proposed mode of operation and was not evaluated as part of this assessment.

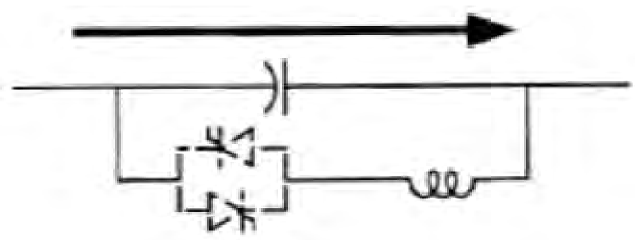

Figure 4-2. TCSC in Blocked Mode

4.1.2 Thyristor Bypassed Mode

In this mode of operation thyristors are continuously fired so they conduct fully in both the positive and negative cycles. Therefore the TCSC offers a value of inductive reactance very close to that of the reactor "L" in parallel with the capacitor C. The choice of "L" and "C" are such that at the fundamental frequency, the parallel combination of "L" and "C" will provide an inductive reactance. Typically if there is an external fault within the network and the line current through the TCR branch is well within the device limit, this mode is used for few cycles after the fault inception. A schematic diagram showing the bypass mode of operation is shown in Figure 4-3. The operational details of Dominion's proposed project are not fully defined in the supplied information, but it is not expected that Dominion TCSCs would operate in this mode.

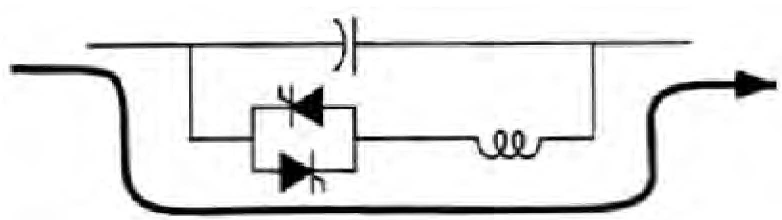

Figure 4-3. TCSC Bypass Mode

4.1.3 Vernier Control Mode

This is the mode of operation primary used in a TCSC installation. The primary objective of this mode is to provide a variable reactance that could be continuously controlled per the needs of connected grid in either the capacitive or inductive range. While being operated in the capacitive zone, a TCSC can provide higher capacitance as compared to installed series capacitance "C" as seen in Figure 4-1. This is called the capacitive boost mode.

Capacitive Boost

If the thyristor is fired a little before the capacitor voltage becomes zero and goes positive. There will be a pulse of circulating current "iV" through the parallel TCR branch that will add to the line current "iL" resulting a higher voltage across capacitor as shown in Figure 4-4.

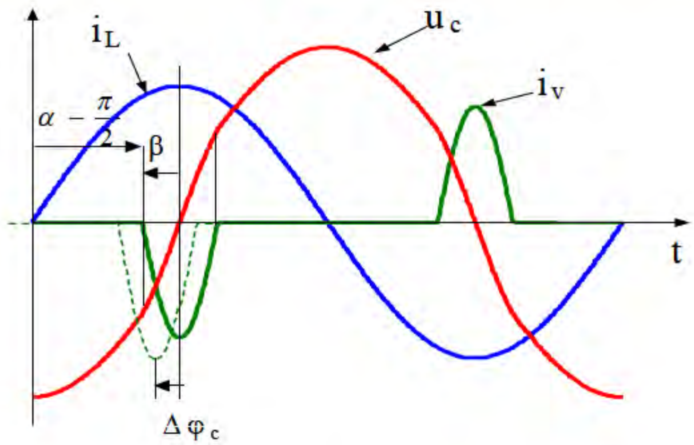

Figure 4-4. Capacitive Boost Mode

Thus the TCSC will provide an effective higher capacitive reactance. The boost factor will be dependent on the firing instant of the thyristors and can be increased by increasing the conduction time through the TCR branch. The effect of increasing the conduction time of the thyristor and resulting capacitor voltage (and thus effective capacitive reactance) is shown in Figure 4-5. Note that the nomenclature is different between Figure 4-4 and Figure 4-5. The Dominion TCSCs would operate in this mode.

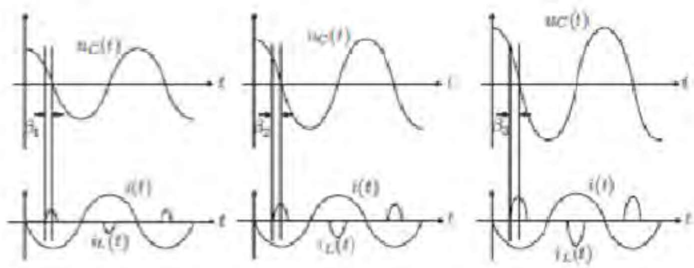

Figure 4-5. Variable TCSC Capacitive Reactance

Inductive Boost

If the thyristor conduction angle is increases beyond a particular value, the TCSC mode changes from capacitive to inductive. In this mode the capacitor voltage gets reduced due to TCR branch current "iV". This mode of operation is shown for various firing angles in Figure 4-6. In general, a TCSC is used in a capacitive mode and not operated in the inductive boost range. The Dominion TCSCs would not operate in this mode.

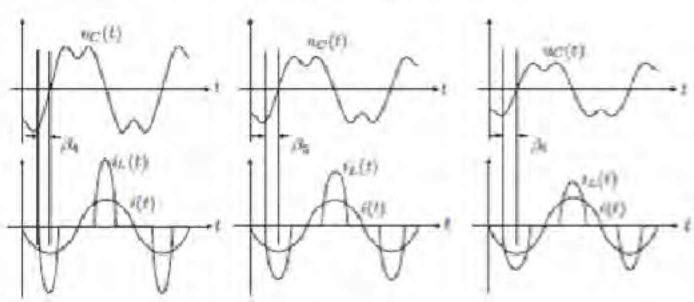

Figure 4-6. Variable TCSC Inductive Reactance

An actual TCSC has many other components such as the MOV, spark gap, bypass circuit etc, as shown in Figure 4-7.

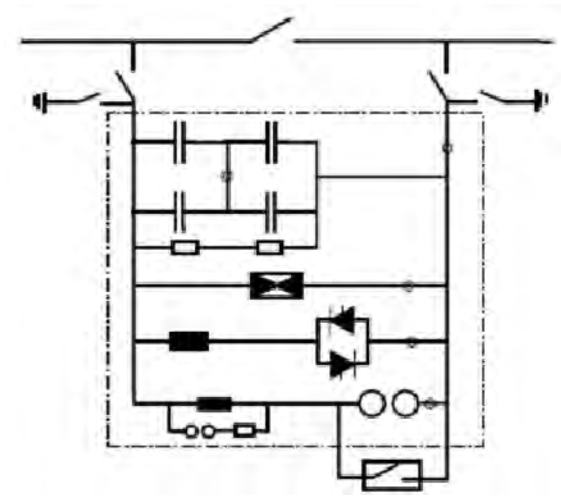

Figure 4-7. TCSC Components

The TCSC's effective reactance was plotted against the firing angle for the Salem – New Freedom line and is shown in Figure 4-8. The details of this TCSC including the main circuit parameters are given in Appendix B. Note that the TCSC appears capacitive for firing angles above 150 degrees or so. The TCSC looks inductive for firing angles below about 140 degrees. There is a range in-between where the circuit is resonant; operation in this region is not allowed. Of course, since the TCSC is generally designed to represent a series capacitor at the fundamental frequency, the firing angles would only be operated in the range above 150 degrees.

Dominion has proposed to operate the two TCSCs in the AI project at a fixed firing angle to compensate a fixed percentage of the connected line's reactance. In this assessment, the two TCSCs in the AI project were modeled at discrete, fixed firing angles. The discrete firing angles for each TCSC were calculated to produce the discrete pre-contingency impedance of 40% and 45% respectively for normal operation, and to produce 90% impedance for both TCSCs for a limited duration in post-contingency operation. The TCSC parameters and firing angles are explained in more detail in the following section.

[redacted]

Figure 4-8. Salem -New Freedom TCSC Characteristic

4.2 Details of the TCSCs in the Artificial Island

The project proposed by Dominion Virginia Power “Proposal -1A” includes installation of two TCSCs as follows:

1. Salem – New Freedom Line (line reactance is 30Ω):

    a. Pre-contingent series compensation needed is 45%. TCSC needs to provide 13.5Ω

    b. Post-contingent series compensation needed is 90%. TCSC needs to provide 27Ω

2. Hope Creek – New Freedom Line (line reactance is 26.25 Ω):

    a. Pre-contingent series compensation needed is 40%. TCSC needs to provide 10.5Ω

    b. Post-contingent series compensation needed is 90%. TCSC needs to provide 23.25Ω

The equipment designer selects the values of the L and C of the TCSC and the related firing control logic to get the desired characteristic. Specific design details of the proposed TCSCs were not available, other than the overall impedance needed as given above.

The design of the TCSC was not part of the scope of this project, and clearly needs to be performed by the supplier of the TCSC. However, in order to investigate the potential for SSR, it was necessary to have TCSC parameters. Since they were not available, it was necessary to assume parameters for the TCSC's L, C and firing angle. The following section gives parameters that are based on a review of the literature by Siemens PTI and are consistent with general TCSC designs. They do not represent an optimization of the controls or other design parameters. Detailed analysis by manufacturer staff with design experience developed over many TCSC projects may result in different parameters.

4.2.1 Salem – New Freedom TCSC

Considering the minimum capacitive reactance that this TCSC needs to provide determines the value of series capacitor "C". In order to provide 45% compensation, i.e. 13.5 Ω, a boost factor of 1.1 is chosen and that gives the value of C to be 216.14 μF. The value of the TCR reactor L is chosen as 5.2 mH, giving a resonant frequency of approximately 145 Hz. Typically this resonant frequency is between 140 to 150 Hz [2]. For 90% series compensation the boost factor is chosen to be 2.19, giving 27 Ω. The corresponding firing angles are calculated as follows:

- $\alpha = 162.29°$ (45%)
- $\alpha = 149.79°$ (90%)

The TCSC parameters are summarized in Appendix B.

4.2.2 Hope Creek – New Freedom TCSC

Considering the minimum capacitive reactance that this TCSC needs to provide will determine the value of series capacitor "C". In order to provide 40% compensation, i.e. 10.5 Ω, a boost factor of 1.1 is chosen and that gives the value of C to be 277.89 μF. The value of the TCR reactor L is chosen as 4.1mH, giving a resonant frequency of approximately 144 Hz. For 90% series compensation the boost factor is chosen to be 2.43, giving 23.25 Ω. The corresponding firing angles are calculated as follows:

- $\alpha = 162.29°$ (40%)
- $\alpha = 149.1°$ (90%)

The TCSC parameters are summarized in Appendix B.

4.3 TCSC and Subsynchronous Resonance

Generally speaking a TCSC can help minimize the possibility of undesired SSR interaction with the surrounding network while increasing the power transfer limit [3]. There are two possible approaches to mitigate the SSR interaction. The first is to utilize the inherent damping of subsynchronous oscillations provided by TCSC operating at a fixed firing angle. Ideally the TCSC should offer the exact amount of series compensation (capacitive) at fundamental frequency and appear as an inductive element while being excited at subsynchronous frequencies. It has also been shown in [5] that a TCSC can offer a resistive damping effect at subsynchronous region and thereby mitigates SSR. However performance depends also on the surrounding networks. Therefore one cannot say for certain unless a detailed analysis is carried out to evaluate all of the pertinent scenarios. Within the proposed "Project -1A" by Dominion Virginia Power, the TCSCs are expected to operate at two fixed firing angles providing a fixed pre-contingent compensation and another higher fixed post-contingent (for limited time only) compensation.

The second approach to minimize the potential for SSR is to design and implement an active close loop damping controller. In this approach the line current is monitored and if SSR oscillations are observed, they are controlled by modulating the compensation level around its operating point to introduce a damping torque [6].

In this study the designed TCSC behavior (two levels of fixed compensation and no modulation) was evaluated at subsynchronous frequencies to see the impact on SSR and the damping of torsional vibrations.

This page intentionally left blank.

Section

5

Contingency Analysis

A set of contingencies were selected that result in radial or near radial connection of the TCSC compensated line(s) and the AI generating unit(s). These contingencies included outage of up to four lines. The loading of the Salem – New Freedom and Hope Creek – New Freedom lines was determined for each of the selected contingencies. The selected contingencies are shown in Table 5-1. These contingences were chosen to maximize the influence of the series compensated lines on the AI units and thus maximize the potential for SSR. The change in flow on the series compensated lines is shown as it indicates the impact of the contingency on these lines. The contingencies with the largest change in flow are those where the characteristics of the TCSC are most critical.

It is noted that the outage of the three circuits, viz. Salem – Orchard, Salem – Hope Creek, and Hope Creek – Red Lion, would result in a loading of [redacted] of the N-0 rating of the Salem – New Freedom line. This outage results in the Hope Creek unit connected radially to New Freedom through one of the series compensated lines and the two Salem units connected radially to New Freedom through the other series compensated line. The power flow results for this contingency showing the network around the AI units are displayed in Figure 5-1.

Further, the outage of the two circuits, viz. Salem – Orchard and Hope Creek – Red Lion, would result in a loading of [redacted] on the Hope Creek – New Freedom line. This outage results in the Hope Creek unit and both Salem units connected radially to New Freedom through the two series compensated lines. The power flow results for this contingency showing the network around the AI units are shown in Figure 5-2.

Additional radial and outage scenarios suggested by PJM were also investigated and their impacts on the branch loadings of the TCSC compensated lines are presented in Table 5-2. The power flow results for the additional radial scenarios B1 to B6 are presented in Figure C 1 through Figure C 6 in Appendix C. Note that the Additional Radial Scenario B7 in Table 5-2 is identical to Scenario A7 in Table 5-1. Also note that PJM uses line numbers to represent the AI lines as compared to using the terminal substation names as given above. A legend is added to Table 5-2 for those not familiar with the line numbering.

Variations of the additional Radial Scenario 7 are created by considering the outage of the two of the three units in the AI. The branch loadings for the corresponding three scenarios are displayed in Table 5-3 and their power flow results are presented in Figure C 7 through Figure C 9 in Appendix C.

The radial and outage scenarios that connect only one generating unit to the TCSC lines were selected for evaluation of SSR issues. These scenarios are:

Scenario SSR1. [redacted]
Scenario SSR2. [redacted]
Scenario SSR3. [redacted]
Scenario SSR4. [redacted]
Scenario SSR5. [redacted]
Scenario SSR6. [redacted]

Table 5-1. AI Area Contingency Scenarios

Transmission Line:		Salem - New Freedom	Hope Creek - New Freedom	Salem - New Freedom	Hope Creek - New Freedom
		Base Case Power Flow in MW		Branch Loading in % (Rate A)	
	Base Case	[redacted]	[redacted]	[redacted]	[redacted]
Scenario Number	Contingency Description	Change in Power Flow in MW (Δ from Base Case)		Branch Loading in % (Rate A)	
A1	[redacted]	[redacted]	[redacted]	[redacted]	[redacted]
A2	[redacted]	[redacted]	[redacted]	[redacted]	[redacted]
A3	[redacted]	[redacted]	[redacted]	[redacted]	[redacted]
A4	[redacted]	[redacted]	[redacted]	[redacted]	[redacted]
A5	[redacted]	[redacted]	[redacted]	[redacted]	[redacted]
A6	[redacted]	[redacted]	[redacted]	[redacted]	[redacted]
A7	[redacted]	[redacted]	[redacted]	[redacted]	[redacted]

Table 5-2. Additional Radial and Outage Scenarios

Additional Scenario Number	500 kV Line Outage Conditions in the AI Area	Notes	Branch Loading in %	
			Salem - New Freedom	Hope Creek - New Freedom
B1	[redacted]	[redacted]	[redacted]	[redacted]
B2	[redacted]	[redacted]	[redacted]	[redacted]
B3	[redacted]	[redacted]	[redacted]	[redacted]
B4	[redacted]	[redacted]	[redacted]	[redacted]
B5	[redacted]	[redacted]	[redacted]	[redacted]
B6	[redacted]	[redacted]	[redacted]	[redacted]
B7	[redacted]	[redacted]	[redacted]	[redacted]

Legend

Line # 5015 – Hope Creek – Red Lion
Line # 5021 – Salem – Orchard
Line # 5023 – Hope Creek – New Freedom
Line # 5024 – Salem – New Freedom
Line # 5037 – Salem – Hope Creek
Line # 5038 – New Freedom – East Windsor
Line # 5039 – New Freedom – Orchard

Table 5-3. Radial Scenarios:
One Generating Unit with Two TCSC Lines

No	500 kV Line Outage Conditions in the AI Area	Notes	Branch Loading in %	
			Salem - New Freedom	Hope Creek - New Freedom
C1	[redacted]	[redacted]	[redacted]	[redacted]
C2	[redacted]	[redacted]	[redacted]	[redacted]
C3	[redacted]	[redacted]	[redacted]	[redacted]

[redacted]

Figure 5-1. Scenario A7: Power Flow in the AI Area following Outage of the Three Circuits: [redacted]

[redacted]

Figure 5-2. Scenario A6: Power Flow in the AI Area following Outage of the Two Circuits: [redacted]

This page intentionally left blank.

Section

6

Development of Network Equivalent in PSCAD

The analysis of the response of the TCSCs and the potential for SSR requires a detailed transient level model and simulation software such as the PSCAD program. This type of analysis does not require representation of the entire PJM grid as, for example, given in the load flow cases discussed in Section 5, but rather a very detailed representation concentrating on the local area. In order to develop a transient model of PJM's network around the AI generating units, the first step was to determine the extent of the network that should be represented by their detailed component models. The appropriate extent of the network was determined through frequency scan analysis and transient simulation.

The network equivalencing procedure comprised the matching of the load flow, the short circuit strength, and the frequency response. The matching of the load flow enabled starting from the correct initial condition for the transient simulation. Similarly, the matching of the short circuit strength helps in assuring that the impact of the external network is appropriately represented in the equivalent model. The matching of the frequency response ensures that the possible resonance conditions are adequately captured by the equivalent model. The dynamic response was checked to ensure a reasonable, but not exact match, of the response in the frequency range of power-angle oscillations.

A frequency scan or impedance-frequency scan presents a visual indication of resonance conditions at a specific bus. The parallel resonances are associated with high impedances to the current flows, and appear as "peaks" in the impedance vs. frequency plot. Series resonances, on the other hand are associated with low impedances to subsynchronous current flows, and appear as "valleys" in the plot.

The search for potential series resonant states of the electrical networks in frequency scan is defined by those points where the system driving point impedance is at a minimum and is transitioning from a capacitive to an inductive state. Thus, the point of a frequency scanning plot of the system impedance is to identify network configurations with potential SSR problems, indicated where the system reactance is zero (series resonant point) or is at a local minimum.

6.1 Frequency Scan Analysis

Four transient models were developed via conversion from the existing steady state and dynamic simulation PSS®E models. These models included system buses up to 4, 5, 6, and 7 buses away from the Salem 500 kV bus. The 500 kV and 230 kV lines, transformers, generators, reactive devices, and loads were part of the transient model. The generator models were based on the PSS®E dynamic simulation database. The transmission system beyond the specified number of buses away from the Salem 500 kV bus was converted to an equivalent network, with fixed voltage sources behind positive sequence equivalent impedances.

The frequency scans obtained the system driving point positive sequence impedance as a function of the network electrical frequency at the terminals of the Salem and Hope Creek generating units. The frequency scan was performed for the subsynchronous range of frequencies.

The TCSC was represented as a series capacitor for the purpose of the frequency scan analysis. It should be noted that due to thyristor switching, the TCSC would not have the frequency response of a fixed series capacitor, but can behave as either an inductive reactance or a capacitive reactance in the subsynchronous frequency range depending on the TCSC parameters and firing angle. However, representing the TCSC as a series capacitor for the frequency scans is adequate to show the impact of the various levels of system representation.

The frequency scans were obtained for two levels of compensation of the Salem – New Freedom and Hope Creek – New Freedom lines. The following operating scenarios were considered:

1. No contingency
2. Three circuit outage: [redacted]
3. Two circuit outage: [redacted]

The frequency scans are compared for the four transient models (4, 5, 6, and 7 buses away from the Salem 500 kV bus) in Figure 6-1 through Figure 6-7. The frequency scans are given for both the impedance seen at the terminals of Salem Unit 2 and Hope Creek unit (Salem Unit 1 would be similar). It can be observed that for all operating scenarios, the frequency responses for all the 4 transient models present a similar response. The impedance scan plot reveals the peaks that indicate parallel resonance and the valleys that indicate series resonance. The series and parallel resonant frequencies are identical for all four models. The difference can be seen in the peak magnitude of the positive sequence impedance. The four-bus-away model presents a lower resonant peak as compared to the other 3 models, indicating a higher damping in the case of the 4-bus-away model. The parallel and series resonant frequency results for the 4 models are compiled in Table 6-1 and Table 6-2 respectively. The damping for parallel resonance as reflected in the peak impedance magnitude is almost the same for the 6-bus-away and 7-bus-away models. The impedance magnitudes corresponding to the valleys in the impedance scans are identical for 6-bus-away and 7-bus-away models. Both models capture the same series resonance behavior of the network. Thus, it was determined that the 6-bus-away model is adequate for capturing the system transient response in the subsynchronous range of frequencies and was used for the transient simulations.

[redacted]

Figure 6-1. Frequency Scans at the Terminal of Salem Unit 2 (40/45% SC)

[redacted]

Figure 6-2. Frequency Scans at the Terminal of Salem Unit 2 (40/45% SC)

[redacted]

Figure 6-3. Frequency scans at the Terminal of Salem Unit 2 (90% SC)

[redacted]

Figure 6-4. Frequency Scans at the Terminal of Salem Unit 2 (40/45% SC)

[redacted]

Figure 6-5. Frequency Scans at the Terminal of Hope Creek unit (40/45% SC)

[redacted]

Figure 6-6. Frequency Scans at the Terminal of Salem Unit 2 (90% SC)

[redacted]

Figure 6-7. Frequency Scans at the Terminal of Hope Creek unit (90% SC)

Table 6-1. Parallel Resonance Frequencies

Scenario	Impedance measured at	Degree of Compensation	Parallel Resonance Frequency (Hz)	Peak Impedances ohms			
				4-bus away	5-bus away	6-bus away	7-bus away
No contingency	Salem Unit 2	40/45%	[redacted]				
3 circuit out	Salem Unit 2	40/45%					
3 circuit out	Salem Unit 2	90%					
2 circuit out	Salem Unit 2	40/45%					
2 circuit out	Hope Creek unit	40/45%					
2 circuit out	Salem Unit 2	90%					
2 circuit out	Hope Creek unit	90%					

Table 6-2. Series Resonance Frequencies

Scenario	Impedance measured at	Degree of Compensatio n	Series Resonance Frequency (Hz)	Impedance (corresponding to the valley) ohms			
				4-bus away	5-bus away	6-bus away	7-bus away
No contingency	Salem Unit 2	40/45%	[redacted]				
3 circuit out	Salem Unit 2	40/45%					
3 circuit out	Salem Unit 2	90%					
2 circuit out	Salem Unit 2	40/45%					
2 circuit out	Hope Creek unit	40/45%					
2 circuit out	Salem Unit 2	90%					
2 circuit out	Hope Creek unit	90%					

6.2 Model Validation

A PSCAD model of the PJM network around the AI generator was developed by retaining all system buses up to 6 buses away from the Salem 500 kV bus. The data conversion from the PSS®E base cases to PSCAD format was performed by converting the steady-state power flow case using the E-TRAN program. The system model included the dynamic models of the generators and their control systems at Salem Unit 1, Salem Unit 2, Hope Creek unit, Peach Bottom-2, and Peach Bottom-3. The parameters of these models were based on the machine and controller parameters available in the PSS®E dynamic data base. The sequence parameters of the transmission lines were also incorporated in the PSCAD model. The transmission lines were represented by their Bergeron model.

6.2.1 Steady State Validation

The PSCAD model was validated by comparing the steady state results with the results of the PSS®E power flow case. The power flow results for the N-2 operating scenario corresponding to the outage of Hope Creek – Red Lion and Hope Creek – Salem are presented in Table 6-3 and Table 6-4 for some of the buses modeled in the PSCAD representation. From the comparison table, it can be seen that the bus voltages and phase angles at the buses modeled in PSCAD are a close match to the system conditions shown in the PSS®E power flow case. The power outputs of the AI generators also show a close match.

Table 6-3. Comparison of Steady State Conditions

Bus	Voltage Level	PSS®E		PSCAD	
		Voltage (pu)	Phase (Deg)	Voltage (pu)	Phase (Deg)
Alburtis	500	1.0542	-25.89	1.0542	-25.876
Deans	500	1.0561	-31.27	1.056	-31.25
Keeney	500	1.0432	-27.59	1.043	-27.58
New Freedom	500	1.0369	-21.43	1.037	-21.42
Peach Bottom	500	1.05	-24.15	1.05	-24.14
Salem	500	1.038	-16.83	1.038	-16.82
3 Mile Island	500	1.0592	-23.43	1.059	-23.41
Red Lion	500	1.0425	-27.96	1.0425	-27.95
Hope Creek	500	1.0364	-17.17	1.0367	-17.16
Rock Spring	500	1.0486	-24.96	1.0486	-24.92

Table 6-4. Comparison of Steady State Power Output of the AI generators in PSS®E and PSCAD Models

Generator	PSS®E		PSCAD	
	P(MW)	Q(Mvar)	P(MW)	Q(Mvar)
Salem Unit 1	1253	160	1254	158.9
Salem Unit 2	1245	230	1245.6	229.8
Hope Creek unit	1320	241	1321.9	240.9

6.2.2 Short Circuit Results Validation

The Automatic Sequencing Fault Calculation (ASCC) activity of PSS®E was used to determine the 3-phase fault currents at the Salem, Hope Creek, Red Lion and Alburtis 500 kV buses. In order to validate the PSCAD model, three-phase faults were simulated at these buses using the PSCAD representation, and the calculated short circuit currents were compared with the fault currents calculated using PSS®E. This comparison is presented in Table 6-5. As can be seen in the comparison table, the short circuit levels in PSCAD are very close to those determined by PSS®E.

Table 6-5. Comparison of Short Circuit Values in PSS®E and PSCAD Models

Bus	Voltage Level	PSS®E	PSCAD
		3-ph Fault Current	
		Irms (kA)	Irms (kA)
Salem	500 kV	27.8	28.4
Hope Creek	500 kV	17.4	17.6
Red Lion	500 kV	12.7	12.8
Alburtis	500 kV	28	27.9

6.3 Transient Model Performance

As part of the model validation process, the dynamic response of the PSCAD model was also compared to that for the PSS®E model. In the simulations, it was assumed that [redacted] A single-phase to ground fault was simulated on the Salem – Orchard 500 kV line near Salem. The fault was initiated at 1 second and cleared after [redacted] cycles by opening [redacted] This fault resulted in the 3-circuit outage scenario, a very severe contingency for the Salem generating units. The TCSC is modeled as a fixed capacitor for this transient simulation. The detailed model of the TCSC with its firing logic was incorporated later in the PSCAD model for the simulations to study the impact of the TCSC on the AI generating units.

The transient performance of the AI units as obtained from the PSCAD model are presented in Figure 6-8 through Figure 6-10. These plots include the speed, field voltage, electrical and mechanical torques, terminal voltage, and active and reactive power outputs of the Salem Unit 1, Salem Unit 2, and Hope Creek generating unit. The model shows a stable response, relatively similar to the PSS®E model response. The results as obtained from PSS®E simulation are included after Figure 6-10. It should be noted that the intent here is not to develop an equivalent for transient stability analysis, for which a larger model size would be required. While the PSCAD model should appropriately represent the power-angle swings modes, the phenomenon to be studied with the PSCAD model involves subsynchronous frequencies much higher than the oscillation frequencies simulated in PSS®E transient stability analysis.

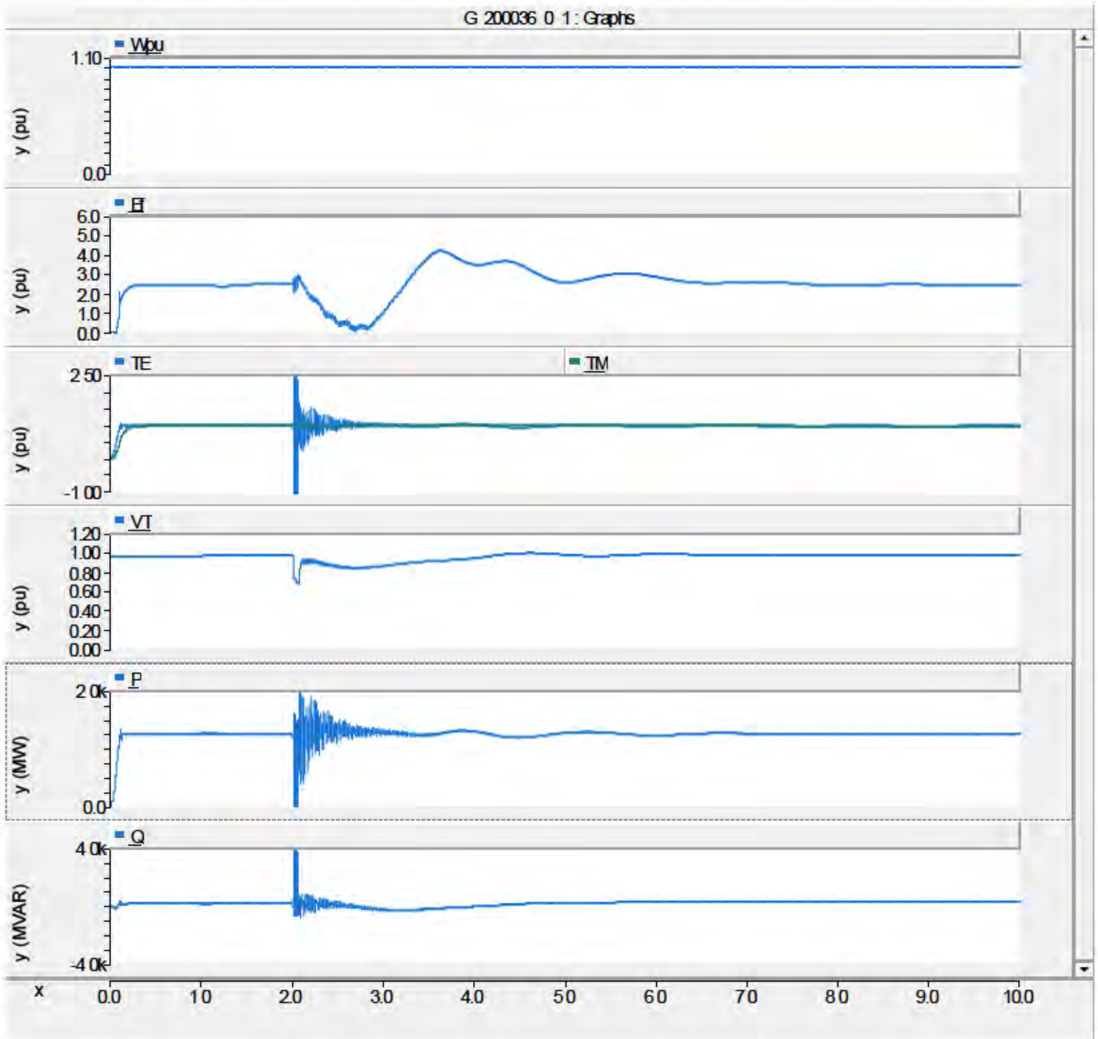

Figure 6-8. Transient Responses of Salem Unit 1 for Single Line to Ground Fault Simulation

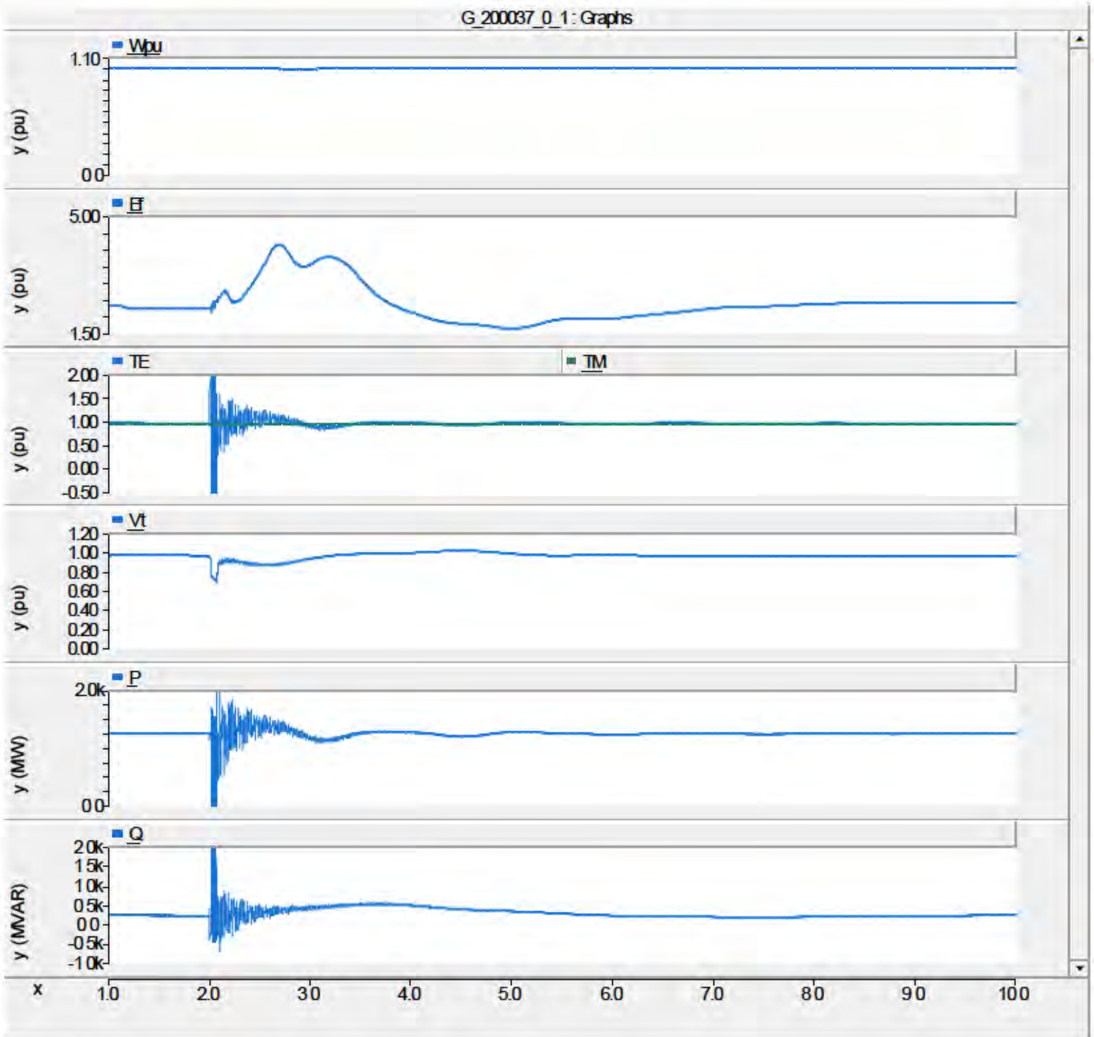

Figure 6-9. Transient Responses of Salem Unit 2 for Single Line to Ground Fault Simulation

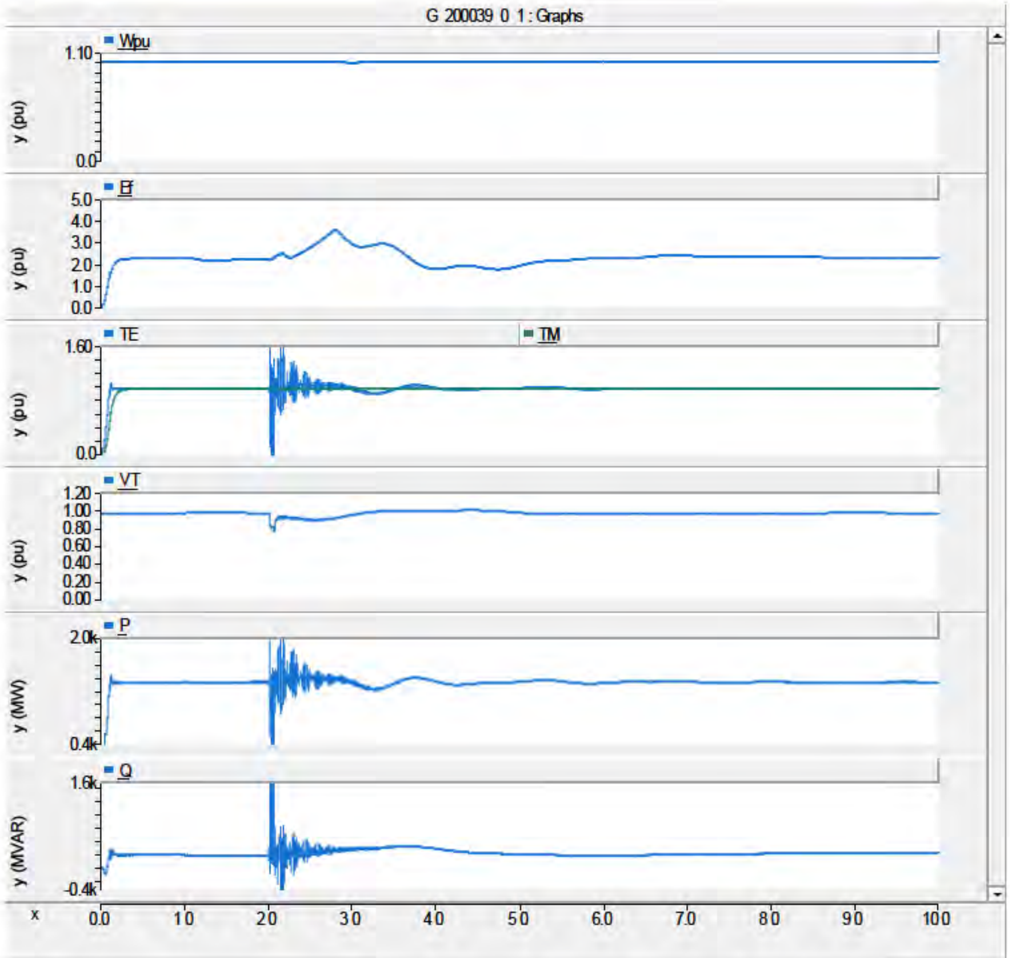

Figure 6-10. Transient Responses of Hope Creek Unit for Single Line to Ground Fault Simulation

6.4 6-Bus-Away PSCAD Model

The one-line diagram of the 6-bus-away PSCAD model is shown in Figure D 1 through Figure D 5 in Appendix D. The PSCAD models of the generators and associated controls for the Salem Unit1, Salem Unit 2, and Hope Creek turbo-generator unit are presented in Figure D 6 through Figure D 8

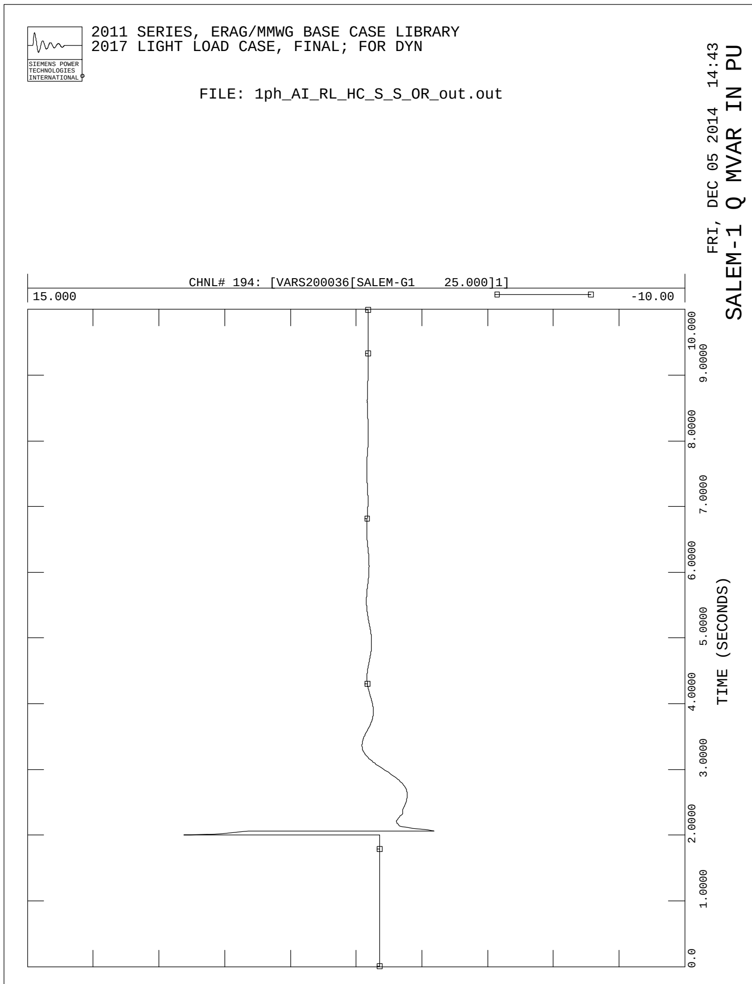
2011 SERIES, ERAG/MMWG BASE CASE LIBRARY
2017 LIGHT LOAD CASE, FINAL; FOR DYN
SIEMENS POWER TECHNOLOGIES INTERNATIONAL
FILE: 1ph_AI_RL_HC_S_S_OR_out.out
FRI, DEC 05 2014 14:43
SALEM-1 Q MVAR IN PU
CHNL# 194: [VARS200036[SALEM-G1 25.000]1]
15.000
-10.00
TIME (SECONDS)
0.0
1.0000
2.0000
3.0000
4.0000
5.0000
6.0000
7.0000
8.0000
9.0000
10.000
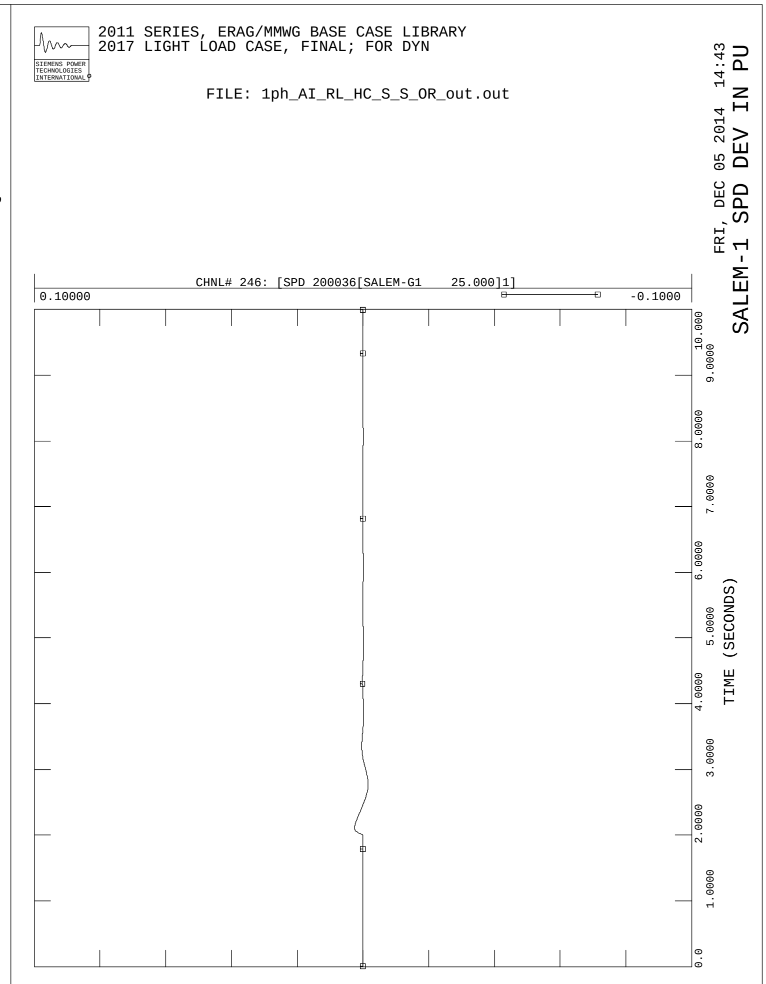
2011 SERIES, ERAG/MMWG BASE CASE LIBRARY
2017 LIGHT LOAD CASE, FINAL; FOR DYN
SIEMENS POWER TECHNOLOGIES INTERNATIONAL
FILE: 1ph_AI_RL_HC_S_S_OR_out.out
FRI, DEC 05 2014 14:43
SALEM-1 SPD DEV IN PU
CHNL# 246: [SPD 200036[SALEM-G1 25.000]1]
0.10000
-0.1000
TIME (SECONDS)
0.0
1.0000
2.0000
3.0000
4.0000
5.0000
6.0000
7.0000
8.0000
9.0000
10.000
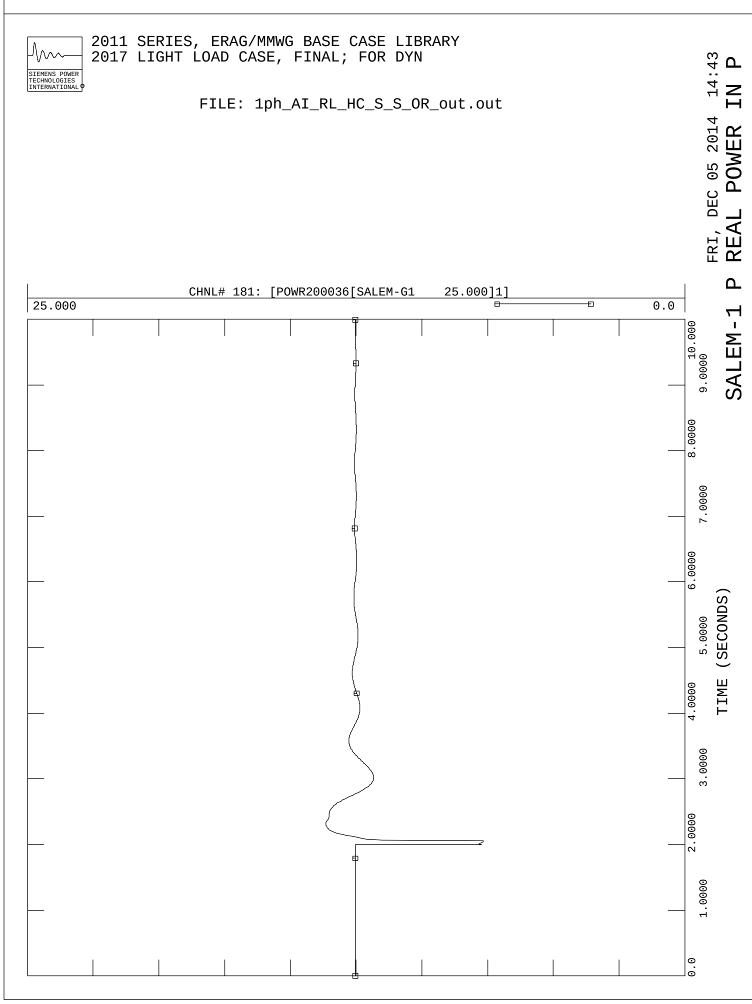
2011 SERIES, ERAG/MMWG BASE CASE LIBRARY
2017 LIGHT LOAD CASE, FINAL; FOR DYN
SIEMENS POWER TECHNOLOGIES INTERNATIONAL
FILE: 1ph_AI_RL_HC_S_S_OR_out.out
FRI, DEC 05 2014 14:43
SALEM-1 P REAL POWER IN P
CHNL# 181: [POWR200036[SALEM-G1 25.000]1]
25.000
0.0
TIME (SECONDS)
0.0
1.0000
2.0000
3.0000
4.0000
5.0000
6.0000
7.0000
8.0000
9.0000
10.000
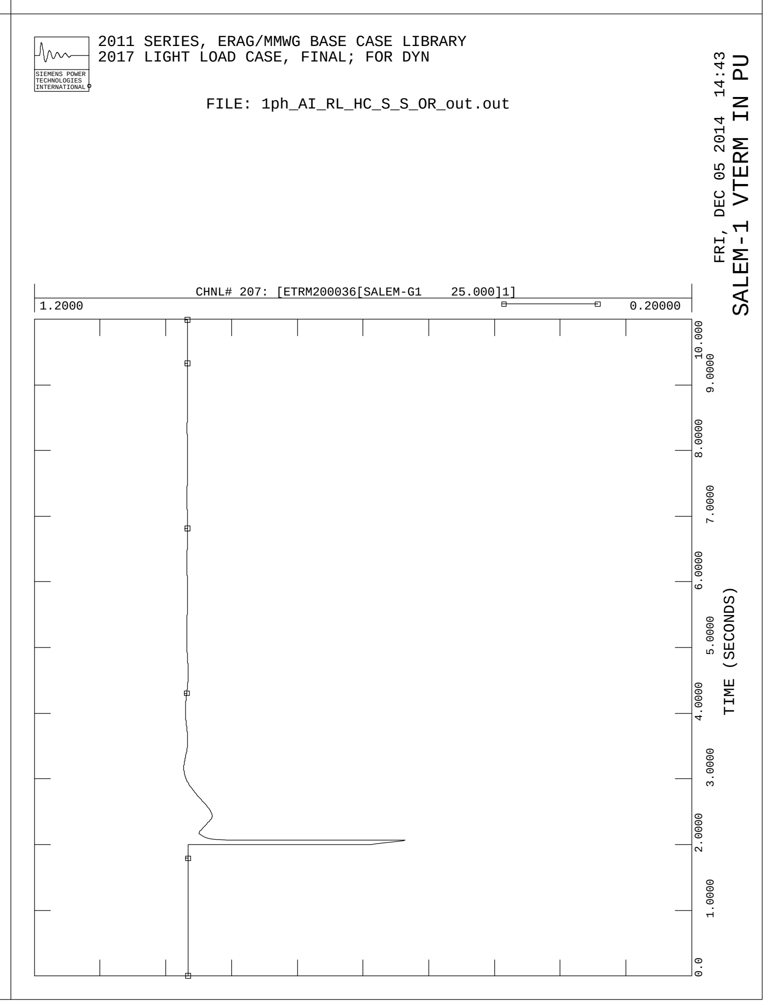
2011 SERIES, ERAG/MMWG BASE CASE LIBRARY
2017 LIGHT LOAD CASE, FINAL; FOR DYN
SIEMENS POWER TECHNOLOGIES INTERNATIONAL
FILE: 1ph_AI_RL_HC_S_S_OR_out.out
FRI, DEC 05 2014 14:43
SALEM-1 VTERM IN PU
CHNL# 207: [ETRM200036[SALEM-G1 25.000]1]
1.2000
0.20000
TIME (SECONDS)
0.0
1.0000
2.0000
3.0000
4.0000
5.0000
6.0000
7.0000
8.0000
9.0000
10.000

2011 SERIES, ERAG/MMWG BASE CASE LIBRARY
2017 LIGHT LOAD CASE, FINAL; FOR DYN

FILE: 1ph_AI_RL_HC_S_S_OR_out.out

FRI, DEC 05 2014 14:43
SALEM-2 Q MVAR IN PU

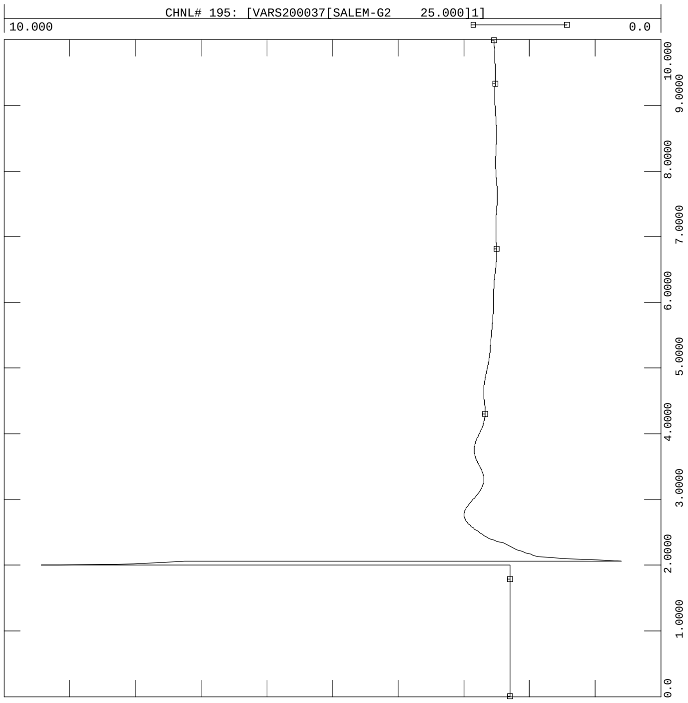

2011 SERIES, ERAG/MMWG BASE CASE LIBRARY
2017 LIGHT LOAD CASE, FINAL; FOR DYN

FILE: 1ph_AI_RL_HC_S_S_OR_out.out

FRI, DEC 05 2014 14:43
SALEM-2 SPD DEV IN PU

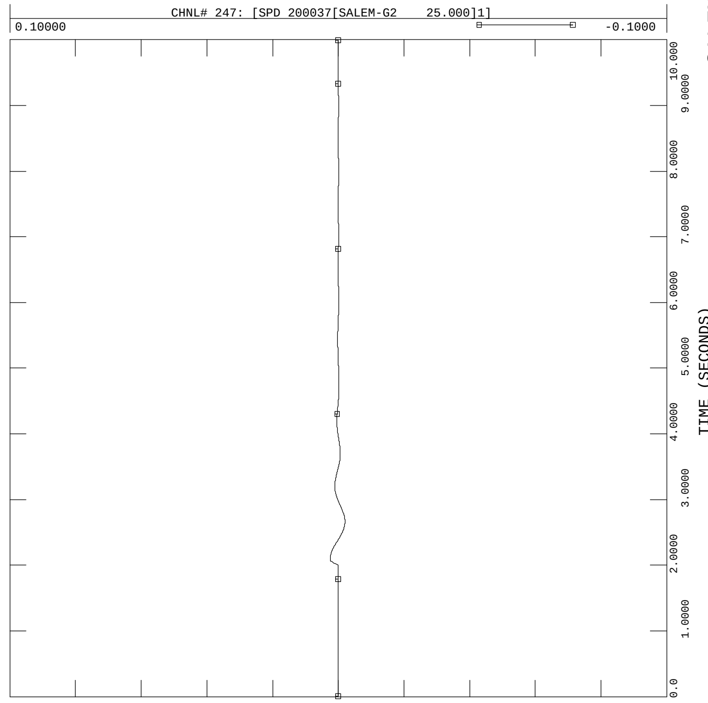

2011 SERIES, ERAG/MMWG BASE CASE LIBRARY
2017 LIGHT LOAD CASE, FINAL; FOR DYN

FILE: 1ph_AI_RL_HC_S_S_OR_out.out

FRI, DEC 05 2014 14:43
SALEM-2 P REAL POWER IN P

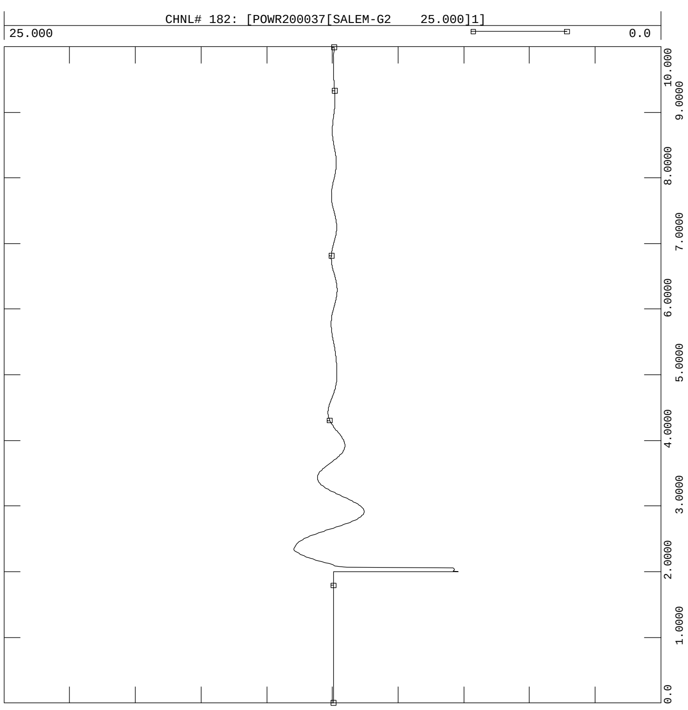

2011 SERIES, ERAG/MMWG BASE CASE LIBRARY
2017 LIGHT LOAD CASE, FINAL; FOR DYN

FILE: 1ph_AI_RL_HC_S_S_OR_out.out

FRI, DEC 05 2014 14:43
SALEM-2 VTERM IN PU

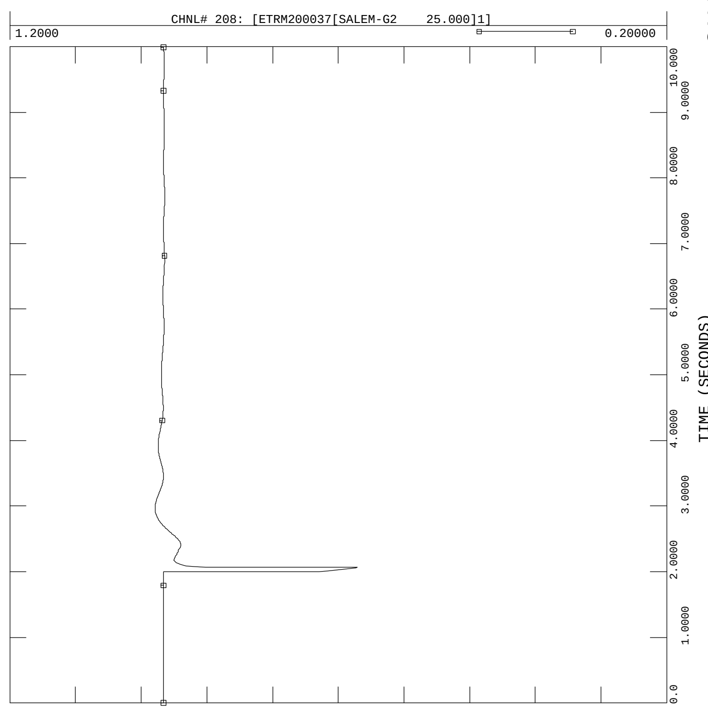

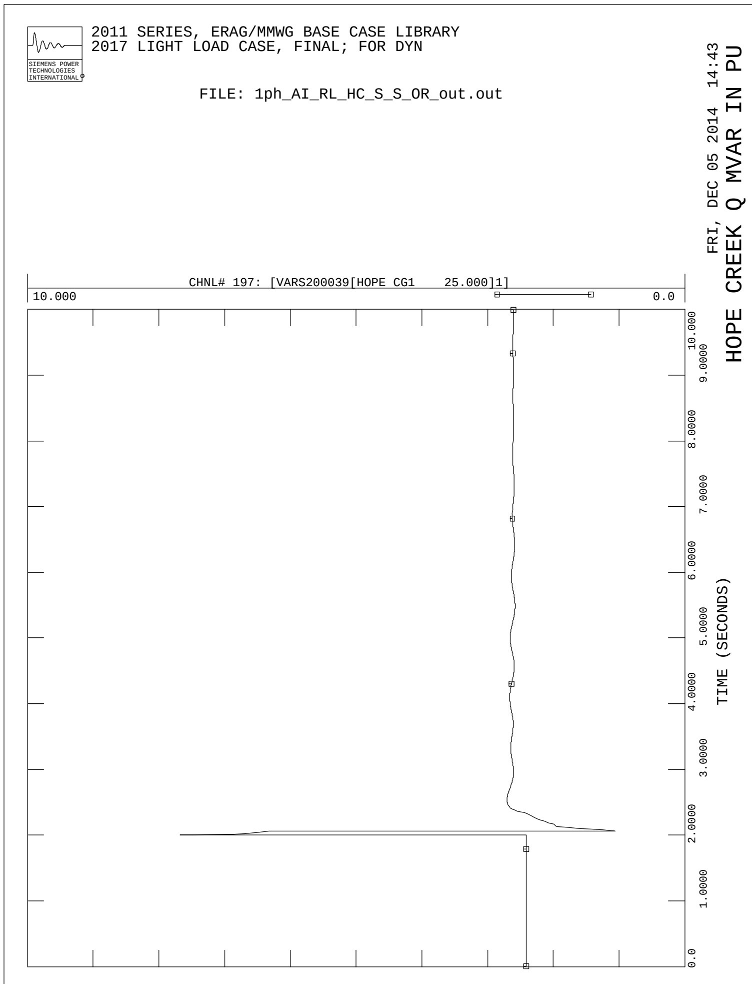
2011 SERIES, ERAG/MMWG BASE CASE LIBRARY
2017 LIGHT LOAD CASE, FINAL; FOR DYN
SIEMENS POWER TECHNOLOGIES INTERNATIONAL
FILE: 1ph_AI_RL_HC_S_S_OR_out.out
CHNL# 197: [VARS200039[HOPE CG1   25.000]1]
10.000
0.0
FRI, DEC 05 2014 14:43
HOPE CREEK Q MVAR IN PU
TIME (SECONDS)
0.0
1.0000
2.0000
3.0000
4.0000
5.0000
6.0000
7.0000
8.0000
9.0000
10.000

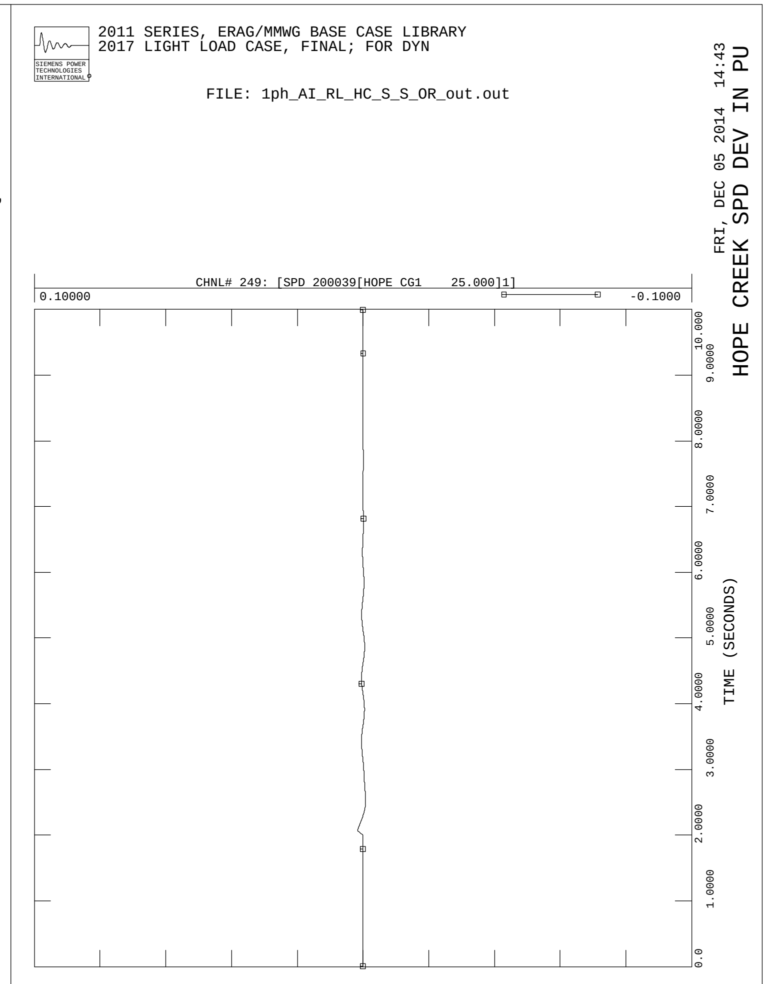
2011 SERIES, ERAG/MMWG BASE CASE LIBRARY
2017 LIGHT LOAD CASE, FINAL; FOR DYN
SIEMENS POWER TECHNOLOGIES INTERNATIONAL
FILE: 1ph_AI_RL_HC_S_S_OR_out.out
CHNL# 249: [SPD 200039[HOPE CG1   25.000]1]
0.10000
-0.1000
FRI, DEC 05 2014 14:43
HOPE CREEK SPD DEV IN PU
TIME (SECONDS)
0.0
1.0000
2.0000
3.0000
4.0000
5.0000
6.0000
7.0000
8.0000
9.0000
10.000

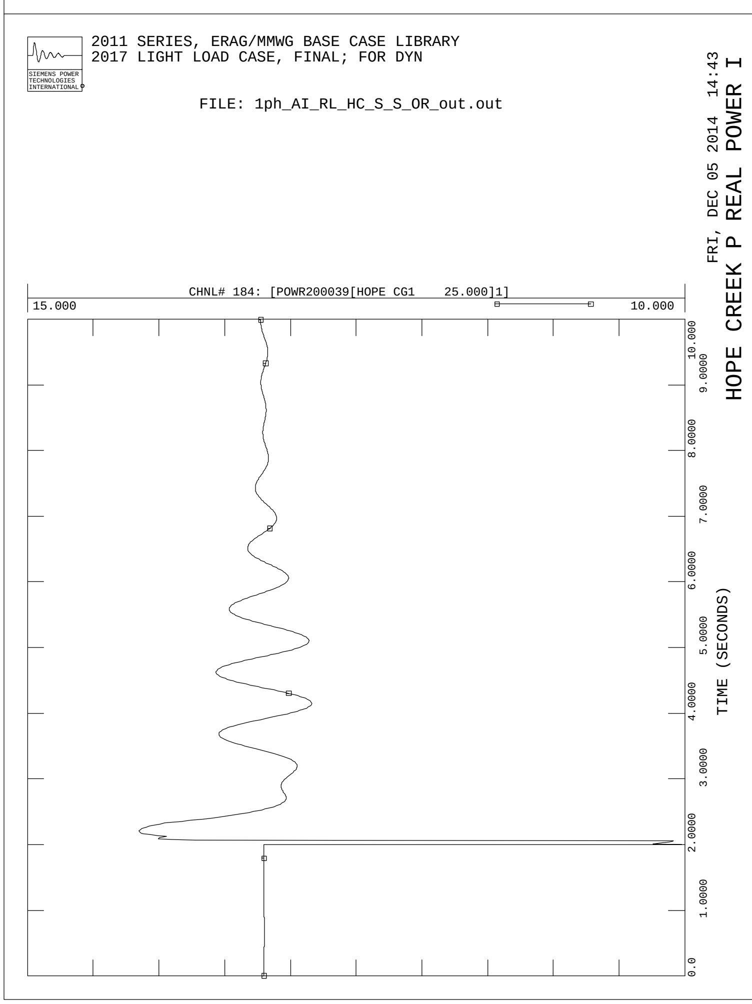
2011 SERIES, ERAG/MMWG BASE CASE LIBRARY
2017 LIGHT LOAD CASE, FINAL; FOR DYN
SIEMENS POWER TECHNOLOGIES INTERNATIONAL
FILE: 1ph_AI_RL_HC_S_S_OR_out.out
CHNL# 184: [POWR200039[HOPE CG1   25.000]1]
15.000
10.000
FRI, DEC 05 2014 14:43
HOPE CREEK P REAL POWER I
TIME (SECONDS)
0.0
1.0000
2.0000
3.0000
4.0000
5.0000
6.0000
7.0000
8.0000
9.0000
10.000

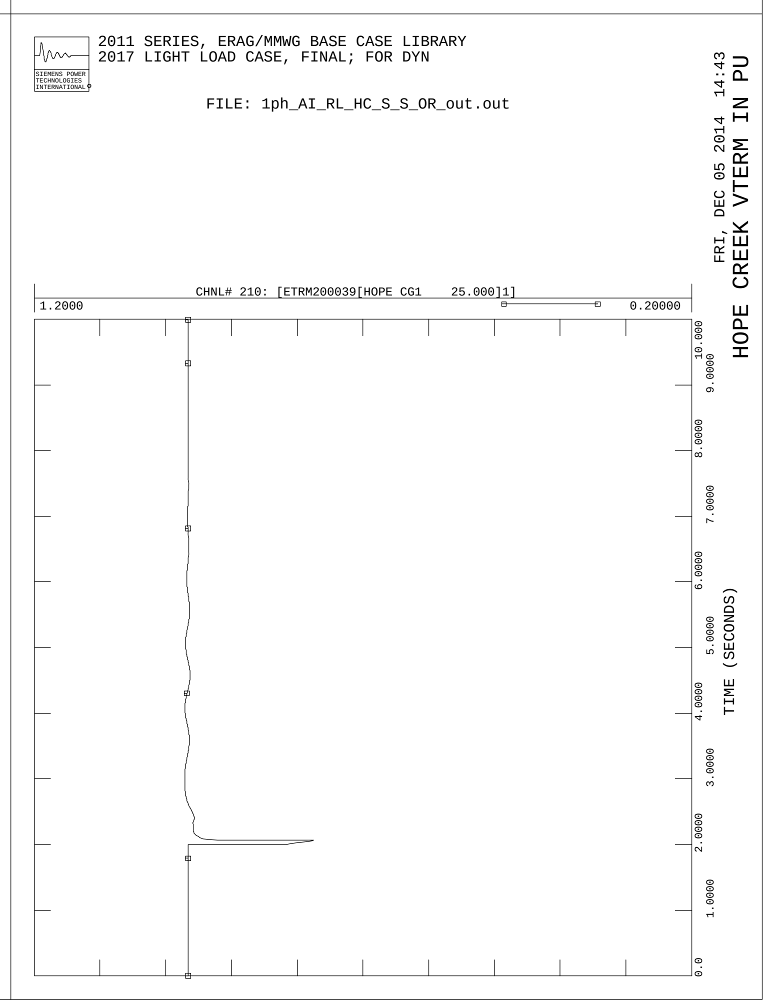
2011 SERIES, ERAG/MMWG BASE CASE LIBRARY
2017 LIGHT LOAD CASE, FINAL; FOR DYN
SIEMENS POWER TECHNOLOGIES INTERNATIONAL
FILE: 1ph_AI_RL_HC_S_S_OR_out.out
CHNL# 210: [ETRM200039[HOPE CG1   25.000]1]
1.2000
0.20000
FRI, DEC 05 2014 14:43
HOPE CREEK VTERM IN PU
TIME (SECONDS)
0.0
1.0000
2.0000
3.0000
4.0000
5.0000
6.0000
7.0000
8.0000
9.0000
10.000

Section 7

TCSC Performance Analysis

The SSR impact of the TCSCs (connected to the Salem – New Freedom and Hope Creek – New Freedom lines) on the AI generating units was determined by simulating a disturbance on the base operating scenario and monitoring the coupling torque in the shaft model.

A small perturbation in the network would be adequate to excite the torsional oscillations on the rotor shafts of the AI generating units. The transient simulations were performed with the PSCAD model of the PJM network by simulating a three phase fault on the Windsor 500 kV bus as shown in Figure 7-1. The fault was applied through an impedance as displayed in Figure 7-2. Note that it is not a solidly grounded three phase fault as typically simulated in transient stability analysis, as here we are looking for the small signal damping characteristics and not the transient stability response.

[redacted]

Figure 7-1. Fault at Windsor

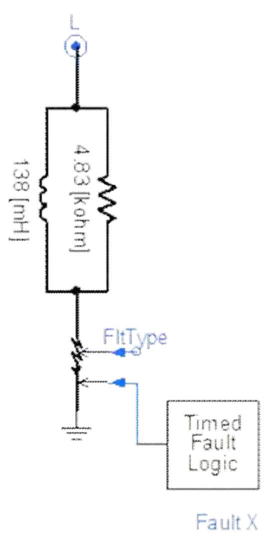

Figure 7-2. Fault Impedance

The fault was applied at 2 seconds after the start of the simulation and the fault was cleared after [redacted] cycles. Each simulation was performed for 10 seconds of simulation time. The simulations were repeated for the selected rotor natural frequencies for each of the generating unit as identified in Section 3.2 and in Appendix A. These studies have considered the nominal compensation of 40/45% on the two lines.

The following radial scenarios were selected for the SSR screening as these scenarios connect the compensated line(s) to only one of the generating units. When only one generating unit is radially connected, the subsynchronous current from the compensated line(s) will flow into only that unit instead of getting distributed amongst several units, thereby having the maximum impact in terms of the potential for exciting SSR.

Scenario SSR1. [redacted]

Scenario SSR2. [redacted]

Scenario SSR3. [redacted]

Scenario SSR4. [redacted]

Scenario SSR5. [redacted]

Scenario SSR6. [redacted]

The generator air-gap torque (TE), turbine torque (TM), and coupling torque were monitored for each of the simulations. The plots for each of the study scenarios are included in Appendix E through Appendix J.

The severity of the initial torque amplitude is governed by the type of the disturbance. The continuation of the torsional oscillations and its damping properties are almost independent of the initial torque amplitude and depend only on the post-event configuration of the power system and the controls.

Three types of responses are observed for the coupling torque

1. Positive damping: the coupling torque amplitude decreases after the initial peak

2. No damping: the coupling torque continues to oscillate with little or no damping

3. Negative damping: the coupling torque amplitudes keeps increasing (subsynchronous resonance)

The “negative damping” response is certainly harmful and can cause immediate shaft damage.

The “No Damping” response of the coupling torque (or similarly very little damping) can also be harmful for the turbo-generators. Since such torsional oscillations can continue for a long time and if the peak torque magnitude exceeds the endurance limit of the material, then each such oscillation adds to the material fatigue. Thus, such oscillations can lead to damage or a reduction in the life of the rotor shaft.

Note that in some cases, the “positive damping” response may also not be an acceptable response. This can be the case if the initial torque amplitude is higher than the endurance limit of the material or if the decay rate is not fast enough, either of which can result in a harmful impact on the rotor shaft.

The two mass rotor model did not include any mechanical damping. The mechanical damping in the actual shaft is small, but always positive. Thus the damping (or negative damping) of the coupling torque oscillations in the simulations is entirely attributed to the interaction with the electrical system.

7.1 Evaluation of the Damping of Coupling Torque Oscillations

The degree of damping of the coupling torque oscillations can be evaluated by determining the logarithmic decrement, LOGDEC. It is determined as follows:

$$LOGDEC = \frac{1}{N}\, ln\left[\frac{A_0}{A_n}\right]$$

where

A_0 and A_n are the peak amplitudes at an initial time t_o and at a later time t_n respectively

$N = f_{rotor}\,(t_n - t_0)$ is the number of cycles between the measurements

The electrical damping torque factor can be evaluated as

$De_i = 2\ Jm_i * fm_i * LOGDEC_i$

where

$$Jm_i = \frac{Jgen}{Jturb}(Jgen + Jturb)$$

The electrical damping is converted into per unit values on a base derived from the generator’s MVA rating

$$De_{base} = 0.9x10^9 x \frac{MVA\ rating}{(\pi\ rpm)^2}$$

The damping was evaluated for each of the rotor natural frequencies of the Salem Unit 1 and Salem Unit 2, and for a range of frequencies for the Hope Creek unit (its rotor natural frequencies were not supplied) for the study scenarios 1 to 6 listed above. The results are presented in Table 7-1 through Table 7-6.

The study results for the Salem Unit 1 show that the electrical damping is positive for the rotor natural frequencies below [redacted] However, the Salem Unit 1 experiences negative damping characteristics for rotor frequencies of [redacted] These observations are made for both operating scenarios evaluated, i.e., Salem Unit 1 radial with 5023 and 5024, and Salem Unit 1 radial with 5024. It should be further noted that when Salem Unit 1 was radial with two compensated lines, the peak amplitude of the torque is as high as 5 pu as compared to 1.5 pu in the scenario with only one compensated line. Thus, it is observed that radial connection with two lines has more adverse impact as compared to the radial connection with only one line.

The study results for the Salem Unit 2 show a positive damping for rotor natural frequencies of [redacted] The damping for the rotor frequencies of [redacted] is a very small positive damping. The coupling torque exhibits sustained oscillations with practically no damping. The study scenario of Salem Unit 2 radial with 5024 shows a negative damping for a rotor resonance frequency of [redacted]

As noted above, the rotor natural frequencies for the Hope Creek unit were not supplied so a range of frequencies was analyzed. The study results for the Hope Creek unit show positive damping for rotor frequencies below [redacted] The electrical damping observed is very small for frequencies between [redacted] The Hope Creek unit experiences negative damping for rotor frequencies higher than [redacted]. The negative damping is significantly higher for a rotor frequency of [redacted] for the scenario of Hope Creek unit radial with 5023 and 5024 and for the rotor frequency of [redacted] for the scenario of Hope Creek unit radial with 5023 only.

The study results have shown that the generating units at the Artificial Islands can be subjected to SSR phenomenon when a TCSC is employed as presently proposed by Dominion. More detailed design analysis by a manufacturer may be able to develop parameters and controls that are less susceptible to SSR, but the initial investigations performed in this analysis could not determine parameters and controls that would result in adequate damping over the entire frequency range of concern and for all potential operating conditions. The design of the TCSCs with respect to their impact on the potential for SSR is technically challenging as it must address several compensation levels (normal and post-contingency compensation levels for both TCSCs and the combinations of these), a range of system conditions including combinations of transmission line and generating unit outages, and the different shaft torsional frequencies of the three AI generating units.

Note that the study did not consider a subsynchronous damping controller (SSDC). An SSDC could have a significant impact on the damping of SSR oscillations and could potentially remedy the concerns seen in the simulations performed. The impact of an SSDC should be evaluated if such a controller can be implemented as part of the proposed TCSCs.

Table 7-1. Scenario SSR1: [redacted]

Rotor Frequency (Hz)	DE_PU	Comment
[redacted]	[redacted]	Positive damping
[redacted]	[redacted]	Positive damping
[redacted]	[redacted]	Little or no damping
[redacted]	[redacted]	Little or no damping
[redacted]	[redacted]	Negative damping
[redacted]	[redacted]	Negative damping (peak torque amplitude ≈ 5 pu)
[redacted]	[redacted]	Negative damping

Table 7-2. Scenario SSR2: [redacted]

Rotor Frequency (Hz)	DE_PU	Comment
[redacted]	[redacted]	Positive damping
[redacted]	[redacted]	Positive damping
[redacted]	[redacted]	Little or no damping
[redacted]	[redacted]	Little or no damping
[redacted]	[redacted]	Little or no damping

Table 7-3. Scenario SSR3: [redacted]

Rotor Frequency (Hz)	DE_PU	Comment
[redacted]	[redacted]	Positive damping
[redacted]	[redacted]	Positive damping
[redacted]	[redacted]	Little or no damping
[redacted]	[redacted]	Little or no damping
[redacted]	[redacted]	Little or no damping
[redacted]	[redacted]	Little or no damping
[redacted]	[redacted]	Negative damping
[redacted]	[redacted]	Negative damping
[redacted]	[redacted]	Negative damping
[redacted]	[redacted]	Negative damping (SSR)
[redacted]	[redacted]	Negative damping (peak torque amplitude ≈ 3 pu)

Table 7-4. Scenario SSR4: [redacted]

Rotor Frequency (Hz)	DE_PU	Comment
[redacted]	[redacted]	Positive damping
[redacted]	[redacted]	Positive damping
[redacted]	[redacted]	Little or no damping
[redacted]	[redacted]	Little or no damping
[redacted]	[redacted]	Negative damping (peak torque amplitude ≈ 1.5 pu)
[redacted]	[redacted]	Negative damping
[redacted]	[redacted]	Negative damping

Table 7-5. Scenario SSR5: [redacted]

Rotor Frequency (Hz)	DE_PU	Comment
[redacted]	[redacted]	Positive damping
[redacted]	[redacted]	Positive damping
[redacted]	[redacted]	Little or no damping
[redacted]	[redacted]	Little or no damping
[redacted]	[redacted]	Negative damping

Table 7-6. Scenario SSR6: [redacted]

Rotor Frequency (Hz)	DE_PU	Comment
[redacted]	[redacted]	Positive damping
[redacted]	[redacted]	Positive damping
[redacted]	[redacted]	Little or no damping
[redacted]	[redacted]	Little or no damping
[redacted]	[redacted]	Little or no damping
[redacted]	[redacted]	Little or no damping
[redacted]	[redacted]	Little or no damping
[redacted]	[redacted]	Negative damping
[redacted]	[redacted]	Negative damping (SSR)
[redacted]	[redacted]	Negative damping
[redacted]	[redacted]	Negative damping (peak torque amplitude ≈ 2.3 pu)

Section

8

Conclusions and Recommendations

Siemens PTI developed a detailed model of the PJM network around the AI generating units in PSCAD to investigate the potential for SSR related to the addition of the two TCSCs which are part of Dominion's proposed solution to the system performance issues related to the AI units. The model was validated by comparing the steady state power flow, short circuit levels and transient stability results to those of the full PJM load flow and stability models.

Several contingency scenarios were created that result in a radial connection of the AI generating units to the TCSC lines. Such radial connections are the conditions most likely to exhibit SSR.

Detailed simulation studies were performed for the proposed project to calculate the damping of torsional oscillations that could be experienced by the AI units. The damping was evaluated for each of the rotor natural frequencies of the Salem Unit 1 and Salem Unit 2, and for a range of frequencies for the Hope Creek unit (its rotor natural frequencies were not supplied).

It has been found that with a set of TCSC parameters developed by Siemens PTI, the system with the TCSCs does not provide positive damping for all subsynchronous frequencies and hence shows the potential for SSR.

The study results for the Salem Unit 1 show that the electrical damping is positive for the rotor natural frequencies below [redacted] However, the Salem Unit 1 experiences negative damping characteristics for rotor frequencies of [redacted] These observations are made for both operating scenarios evaluated, i.e., Salem Unit 1 radial with 5023 and 5024, and Salem Unit 1 radial with 5024. It should be further noted that when Salem Unit 1 was radial with two compensated lines, the peak amplitude of the torque is as high as 5 pu as compared to 1.5 pu in the scenario with only one compensated line.

The study results for the Salem Unit 2 show a positive damping for rotor natural frequencies of [redacted] The damping for the rotor frequencies of [redacted] is a very small positive damping. The coupling torque exhibits sustained oscillations with practically no damping. The study scenario of Salem Unit 2 radial with 5024 shows a negative damping for a rotor resonance frequency of [redacted].

As noted above, the rotor natural frequencies for the Hope Creek unit were not supplied so a range of frequencies was analyzed. The study results for the Hope Creek unit show positive damping for rotor frequencies below [redacted] The electrical damping observed is very small for frequencies between [redacted] The Hope Creek unit experiences negative damping for rotor frequencies higher than [redacted]. The negative damping is significantly higher for a rotor frequency of [redacted] for the scenario of Hope Creek unit radial with 5023 and 5024 and for the rotor frequency of [redacted] for the scenario of Hope Creek unit radial with 5023 only.

The study results have shown that the generating units at the Artificial Islands can be subjected to SSR phenomenon when a TCSC is employed as presently proposed by Dominion. Since detailed design parameters were not supplied by Dominion, it was necessary to develop TCSC parameters and firing angle logic to meet the fundamental frequency specifications. Those parameters satisfy the design criteria available in the technical literature. More detailed design analysis by a manufacturer may be able to develop parameters and controls that are less susceptible to SSR, but the initial investigations performed in this analysis could not determine parameters and controls that would result in adequate damping over the entire frequency range of concern and for all potential operating conditions.

Note that the study did not consider a subsynchronous damping controller (SSDC). An SSDC could have a significant impact on the damping of SSR oscillations and could potentially remedy the concerns seen in the simulations performed. The impact of an SSDC should be evaluated if such a controller can be implemented as part of the proposed TCSCs.

Therefore if this project is to proceed, Siemens PTI recommends that PJM have a discussion with Dominion Virginia Power and further engage the potential manufacturers to develop TCSC designs, potentially with an SSDC, that will mitigate SSR and provide adequate damping over the entire frequency range of concern and for all potential operating conditions.

Analysis such as that performed in this study would be required to investigate the effectiveness of any revised proposal.

Appendix

K

References

1. IEEE Subsynchronous Resonance Task Force of the Dynamic System Performance Working Group, Power System Engineering Committee, “First Benchmark Model for Computer Simulation of Subsynchronous Resonance,” IEEE Transactions on Power Apparatus and Systems, vol. PAS-96, no. 5, pp. 1565-1572, Sep./Oct. 1977.

2. “Thyristor based FACTS controllers for electric transmission systems”, R. Mohan Mathur, R. K. Verma, IEEE Press Series on Power Engineering.

3. “Analysis of TCSC Controllers”, R. Lasseter, I. Dobson, W. Sethares, An EPRI Report, January 1996.

4. “An EMTP Study of SSR mitigation using Thyristor Controlled Series Capacitor”, W. Zhu, R. Spee, R. R. Mohler, G. C. Alexander, W. A. Mittelstadt, D. Maratukulam, IEEE Transactions on Power Delivery, Vol. 10. No. 3, July 1995.

5. “Resistive behavior of Thyristor Controlled Series Capacitors at Sub Synchronous Frequencies”, K. Kabiri, S. Henschel, H. W. Dommel, IEEE Transactions on Power Delivery, Vol. 19, No. 1, January 2004.

6. “Impact of TCSC Control Methodologies on Subsynchronous Oscillations”, L.A.S. Pilotto, A. Bianco, W. F. Long, A. A. Edris, IEEE Transactions on Power Delivery, Vol. 18, No. 1, January 2003.

7. “A Discrete State Space Model of SSR Stabilizing Controller Design for TCSC Compensated System”, K. Kabiri, S. Henschel, J. R. Marti, H. W. Dommel, IEEE Transactions on Power Delivery, Vol. 20, No. 1, January 2005.

8. “A supplementary damping controller of TCSC for mitigating SSR”, Xiang Zheng, Zheng Xu, Jing Zhang, Power & Energy Society General Meeting, 2009. PES '09. IEEE, July 2009.

9. “Output feedback SSR damping controller design based on modular discrete-time dynamic model of TCSC”, S.R. Joshi, E.P. Cheriyan, A.M. Kulkarni, IET Generation, Transmission & Distribution, Volume 3, Issue 6, June 2009, p. 561 – 573.

10. “Suppression of subsynchronous resonance using robust H^{∞} TCSC damping controllers”, Li Wang, Chi-Wen Huang, Power Engineering Society 1999 Winter Meeting, IEEE, 1999.

11. “Subsynchronous resonance damping control of thyristor-controlled series capacitor”, Kakimoto, Naoto, Phongphanphanee, A, Power Delivery, IEEE Transactions on (Volume:18 , Issue: 3), pp 1051-1059.

12. “Clarifications of the SSR Mitigation Mechanism of a TCSC”, Naoto Kakimoto, Akihiro Iida, Morihiro Seki, Kazuya Minoyama and Tadasu Takuma, Electrical Engineering in Japan, Vol. 120, No. 4, 1997.

13. "Advance Series Compensation (ASC) Main Circuit and Related Component", G. Juette, P. Luetzelberger, A. Schultz, S. McKenna, D. Torgerson, Proceedings: FACTS Conference 2, Boston, December 1992, EPRI TR-101784, pp 3.4-1 to 3.4-11.

14. "Thyristor Controlled Series Compensation-Equipment Design for Slatt 500kV Installation", J. Urbenek, R. Piwko, D. McDonald, N. Artinez, Proceedings: FACTS Conference 2, Boston, December 1992, EPRI TR-101784, pp 3.4-11 to 3.4-19.

Siemens Industry, Inc.
Siemens Power Technologies International
400 State Street • P.O. Box 1058
Schenectady, New York 12301-1058 USA
Tel: +1 (518) 395-5000 • Fax: +1 (518) 346-2777

www.siemens.com/power-technologies